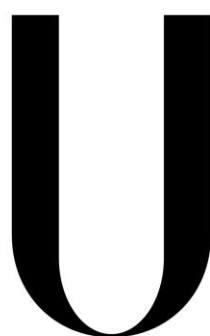


University of Lisbon

Faculty of Sciences

Department of Chemistry and Biochemistry



LISBOA

---

UNIVERSIDADE  
DE LISBOA

**High Temperature Vapour-Liquid Equilibria  
of Water-Polyalcohol mixtures**

**Ana Filipa Russo de Albuquerque Cristino**

PhD in Chemistry

(Specialty in Technological Chemistry)

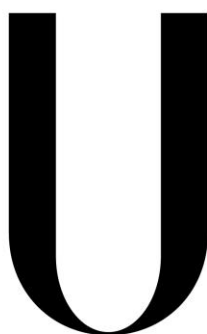
2014



University of Lisbon

Faculty of Sciences

Department of Chemistry and Biochemistry



LISBOA

---

UNIVERSIDADE  
DE LISBOA

**High Temperature Vapour-Liquid Equilibria  
of Water-Polyalcohol mixtures**

Ana Filipa Russo de Albuquerque Cristino

PhD thesis supervised by Professor Carlos Alberto Nieto de Castro and Professor António Manuel Figueiredo Palavra, submitted for the requirements for the degree of Doctor of Chemistry (Specialty in Technological Chemistry)

2014

*“Success is not a place at which one arrives but rather the spirit with which one undertakes and continues the journey.”*

~Alfred Nobel

*To my beloved daughter Madalena*

## Acknowledgements

I would like to acknowledge my supervisors Professor Carlos Castro and Professor António Palavra who transmitted their vast experience and provided useful advices and guidance through all my research and for all the help in the development and orientation of this PhD work.

A word of thanks to Dr. Samuel Rosa, Professors Fernando Santos and Maria José Lourenço who contributed in the construction and maintenance of the equipment used in this thesis.

To Professor Ângela Santos and Msc João Francisco Silva I thank their great help with the distillation of my standards.

I would like also to thank my classmates Ana Paula, Salomé, Carla, Bruno, João França and Beatriz for all the help in the laboratory.

To all of you whose names I don't mention, for all the growing that you gave me , for all the fun times, for every Monday, for all the love and guidance and for having introduced me to my **green** family and more important to my **blue** friends, thank you from the bottom of my heart. Thank you Ana and João, for all the support and help that you weren't obligate to give me. And SMURF POWER!!! 🧪

I thank my family for all the support and my husband for being there for me, even in my worst days. Thank you for taking care of Madalena, who with her excessive egocentric behavior, tried by every means possible, to sabotage the writing of this thesis.

And for the last, I thank all the people who contribute for the administrative work behing this thesis, namely for the acquisition of new material and for calibrations, etc.

## Resumo

Sabe-se que a presença de fortes ligações de hidrogénio no estado líquido cria azeótropos, que desaparecem com o aumento da temperatura. Este comportamento sugere que a destilação a elevadas temperaturas representa uma boa estratégia para separar os componentes de misturas binárias, tais como sistemas de água-álcool, muito relevantes na indústria química.

Os combustíveis biodegradáveis começam a desempenhar um papel importante na economia global do mundo, com os preços do petróleo a aumentar de forma constante, pelo que a busca de energias e de combustíveis alternativos é vital para a sustentabilidade da economia mundial. A produção de combustíveis biodegradáveis como os álcoois requer propriedades de misturas binárias envolvendo álcoois tais como metanol, etanol, propanol, butanol e pentanol (cadeia linear ou ramificada), tanto a partir da experimentação, como da previsão e da correlação. A obtenção de dados de equilíbrio líquido vapour (ELV) a temperaturas elevadas tornou-se um dos meios mais importantes para o dimensionamento de unidades de destilação de alta pressão.

Foi com essa visão que um programa experimental de equilíbrio líquido-vapour (VLE) a elevadas temperaturas foi desenvolvido em colaboração entre o Centro de Ciências Moleculares e Materiais (CCMM - FCUL) e o Laboratório de Termodinâmica Experimental (CQE - IST). As medições de ELV no intervalo de temperaturas 363.3K a 423.7K foram realizadas para os sistemas água+etanol, água+1-propanol e etanol+1-propanol utilizando um aparelho de fluxo.

As medições de ELV a elevadas temperaturas mostram algumas dificuldades experimentais, devido à possível degradação térmica de alguns álcoois, tais como o metanol. Com a finalidade de minimizar este fenómeno, foi escolhido um método de fluxo.

A interpretação teórica destes dados de ELV tem sido feita no passado recorrendo a equações de estado. O sucesso destas interpretações é limitado pelo tipo de

compostos e também pelas condições de trabalho. De entre várias equações de estado, novos métodos que tomam em conta os efeitos de associação molecular têm sido propostos ao longo dos anos. A equação de estado *Statistical Associating Fluid Theory (SAFT)* desenvolvido por Gubbins e colegas é uma delas.

Neste trabalho uma variação dessa equação (*Statistical Associating Fluid Theory for potentials of Variable Range - SAFT-VR*) foi utilizada para prever o ELV das misturas binárias em questão. Esta teoria previu eficazmente o comportamento destas misturas binárias com algumas limitações para alguns componentes puros.

## Abstract

It is known that the presence of strong hydrogen bonds in the liquid state creates azeotropes, which disappear with the increase of temperature. This behavior suggests that the distillation at high temperatures could provide a good strategy to separate components of binary mixtures such as alcohol-water systems, very relevant in the chemical industry.

Biodegradable fuels start to play an important role in the world global economy, as oil prices are increasing steadily and the search for alternative energies and fuels is vital for the sustainability of world economy. The production of biodegradable fuels as alcohols, needs properties of binary mixtures involving methanol, ethanol, propanol, butanol and pentanol (linear and branched), both from experiment, prediction and correlation. High temperature vapour liquid equilibrium (VLE) measurements became one of the key data for the design of high pressure distillation units. Also, alcohols have a wide use in industry as solvents for fats, oils, resins, paints, and nitrocellulose; others find use in the manufacture of perfumes and brake fluids. Mixtures of ethanol with 1-propanol, 1-butanol, or 1-pentanol can be used as fuel oxygenates, as cryogenic fluids and as heat reservoir in cryogenic power generation systems. That's why the knowledge of thermodynamic properties for these mixtures at various temperatures is important.

It was with this vision that a VLE experimental program at high temperatures was developed in a collaboration between the Centre for Molecular Sciences and Materials (CCMM-FCUL) and the Experimental Thermodynamics Laboratory (CQE-IST). The VLE measurements over the temperature range 363.3 K to 423.7 K have been performed for the systems water+ethanol, water+1-propanol and ethanol+1-propanol using a flow apparatus.

The VLE measurements at high temperature show some experimental difficulties due to the possible thermal degradation of some alcohols, like methanol. With the purpose of minimizing this phenomenon, these studies must be carried out using a flow apparatus. This was the main reason for the choice of a flow method over a few types available.



The theoretical interpretation of these VLE data has been done in the past by using equations of state. The success of these interpretations is limited by the type of compounds and also by the working conditions. From the various possibilities, new methods designed to take into account the effects of molecular association have been proposed over the years. The Statistical Associating Fluid Theory (SAFT) equation of state developed by Gubbins and coworkers is one of them.

In this work a variation of this equation (Statistical Associating Fluid Theory for potentials of Variable Range - SAFT-VR) was used to predict the VLE of the binary mixtures in question. This theory was found to accurately predict the behavior of these binary mixtures with some limitations for some pure components.

# Table of Contents

---

|  | <b>Page</b> |
|--|-------------|
| <i>Resumo</i> .....  | <i>i</i>    |
| <i>Abstract</i> .....  | <i>iii</i>  |
| <i>Notation</i> .....  | <i>x</i>    |
| <i>Chapter 1 - Introduction</i> .....  | <i>1</i>    |
| 1.1. Objectives .....  | <i>2</i>    |
| 1.2. Outline of thesis .....   | <i>3</i>    |
| 1.3. Bibliography.....   | <i>4</i>    |
| <i>Chapter 2 - Vapour-Liquid Equilibrium Modeling</i> .....                    | <i>5</i>    |
| 2.1. Introduction .....  | <i>5</i>    |
| 2.2. Thermodynamics of Vapour - Liquid Equilibrium (VLE) .....                 | <i>6</i>    |
| 2.3. Modelling Vapour - Liquid Equilibrium with Equations of State (EOS) ..... | <i>8</i>    |
| 2.3.1. From Van der Waals to SAFT .....  | <i>10</i>   |
| 2.3.2. SAFT EOS.....   | <i>18</i>   |
| 2.4. Bibliography.....   | <i>20</i>   |
| <i>Chapter 3 - VLE Experimental Methods</i> .....                              | <i>23</i>   |
| 3.1. Introduction .....  | <i>23</i>   |
| 3.2. Static Method .....   | <i>25</i>   |
| 3.3. Recirculation Method .....  | <i>26</i>   |
| 3.4. Synthetic Method.....   | <i>28</i>   |
| 3.5. Flow Method .....   | <i>31</i>   |
| 3.6. Bibliography.....   | <i>33</i>   |
| <i>Chapter 4 - VLE apparatus and Experimental Procedure</i> .....              | <i>34</i>   |
| 4.1. Vapour-Liquid Equilibria Apparatus #1 .....                               | <i>34</i>   |
| 4.1.1. Sample feeding section.....   | <i>36</i>   |
| 4.1.2. Equilibrium section .....   | <i>37</i>   |

|   |  |           |
|---|--|-----------|
| 4.1.3.  | Sampling section.....  | 39        |
| 4.2.  | Evaluation and Testing of the VLE Apparatus #1 performance .....                     | 40        |
| 4.2.1.  | LDC Analytical Pump, model 396-74 .....  | 41        |
| 4.2.2.  | Micro-metering Valves .....  | 41        |
| 4.2.3.  | Air Bath.....  | 42        |
| 4.3.  | Vapour-Liquid Equilibria Apparatus #2 .....  | 44        |
| 4.4.  | General operating instructions of the VLE apparatus and experimental procedure ..... | 47        |
| 4.4.1.  | Starting .....   | 48        |
| 4.4.2.  | Equilibrium .....  | 48        |
| 4.4.3.  | Sampling.....  | 48        |
| 4.4.4.  | Turning off.....   | 49        |
| 4.5.  | Bibliography.....  | 49        |
| <i>Chapter 5 – Results and Discussion.....</i>                                |  | <i>50</i> |
| 5.1.  | List of Papers.....  | 50        |
| 5.2.  | Summary of Papers.....   | 51        |
| <i>Chapter 6 – Conclusions and Future Perspectives.....</i>                   |  | <i>79</i> |
| 6.1.  | Overall Comments and Conclusions.....  | 79        |
| 6.2.  | Future Perspectives.....   | 81        |
| 6.3.  | Bibliography.....  | 82        |
| <i>Appendix 1 – Calibrations of the VLE apparatus #1.....</i>                 |  | <i>84</i> |
| A1.1.   | Platinum Resistance thermometer (PT100) from apparatus #1 .....                      | 84        |
| A1.2.   | Manometers from apparatus #1 .....   | 85        |
| A1.1.   | PT100 from apparatus #2 .....  | 87        |
| <i>Appendix 2 – Conversion of densities into molar fractions.....</i>         |  | <i>88</i> |
| A 2.1.  | Bibliography .....   | 89        |
| <i>Appendix 3 – Evaluation of the stability of the air bath of VLE#1.....</i> |  | <i>90</i> |

# Figure Index

---

|   | <b>Page</b> |
|---|-------------|
| Figure 2.1 – Heike Kamerlingh Onnes (left) and van der Waals (right) in front of the helium-<br>‘liquefactor’, Leiden 1908 [13].....  | 11          |
| Figure 2.2 – SAFT-VR model for water (on the left) and alcohol (on the right) .....   | 20          |
| Figure 3.1 – Classification of experimental methods for VLE according to Dohrn <i>et al.</i> [3] .....  | 24          |
| Figure 3.2 – Schematic diagram of a static apparatus for VLE measurements.....  | 25          |
| Figure 3.3 – Schematic of the experimental apparatus of Guo <i>et al.</i> [13]. 1. Feed system; 2.<br>Digital controller; 3. Digital controller; 4. Temperature and pressure indicator; 5. GC; 6 and 7.<br>Motors; 8. Vacuum pump; 9. Vacuum vessel; 10. Cooling coil; 11. isothermal liquid bath; 12.<br>Electric heater; 13. Equilibrium cell; 14. Stirrers; 15. Pressure transducer; 16. N <sub>2</sub> -filled system.<br>.....   | 26          |
| Figure 3.4 Schematic diagram of a recirculation apparatus for VLE measurements.....   | 27          |
| Figure 3.5 - Flowchart of the vapour–liquid equilibrium apparatus Labodest® [14] (1) electrical<br>immersion heater; (2) mixing chamber; (3) contact path; (4) separation chamber; (5) solenoid<br>valves; (6) vapour phase; (7) liquid phase; (8 and 9) circulation steams; (10) sampling port. ...  | 28          |
| Figure 3.6 – Schematic diagram of a synthetic apparatus for VLE measurements.....   | 29          |
| Figure 3.7 - Schematic representation of the new experimental set-up for the measurement of<br>multi-phase equilibria by a synthetic method. (A) High-pressure view cell. (B) Pressure sensor.<br>(C) Platinum resistance thermometers. (D) High-pressure gas cylinder. (E) Data logger. (F) Cold<br>light source with optical fibre (G) Temperature chamber. (H) Stirring with remote control. (I)<br>Video monitor. (J) Video camera. (K) Computer for data acquisition [16]. ..... | 31          |
| Figure 3.8 Schematic diagram of a flow apparatus for VLE measurements .....   | 32          |
| Figure 3.9 –Vapour liquid equilibrium apparatus of Niesen <i>et al.</i> [15] based on a flow method<br>.....  | 32          |
| Figure 4.1 – Schematic of the VLE apparatus #1[1] .....   | 35          |
| Figure 4.2 – Overall view of VLE apparatus #1. A – feeding vessel; B – circulating pump; C –<br>oven with window; D – Measurement and control zone; E – Sampling zone. ....   | 35          |
| Figure 4.3 – Schematic of the sample feeding section of the VLE apparatus #1 [1].....   | 36          |
| Figure 4.4 – Schematic of the equilibrium section of the VLE apparatus #1 [1].....  | 38          |
| Figure 4.5– View of the high pressure cell of VLE apparatus #1 .....  | 38          |
| Figure 4.6 – Schematic of the sampling section of the VLE apparatus #1 [1].....   | 40          |

|   |    |
|---|----|
| Figure 4.7 – Stability of the air bath at 296.55K without any filling or with steel mesh filling in comparison with the temperature measured with the open bath (standard)..... | 43 |
| Figure 4.8 – Stability of the air bath at 423.15K without any filling or with steel mesh in comparison with the PID controller temperature (standard).....                      | 44 |
| Figure 4.9– VLE apparatus #2.....   | 45 |
| Figure 4.10 – a) Frontal view of the high pressure equilibrium cell of the VLE apparatus #2, and b) upper cut view of the cell. ....  | 46 |
| Figure 4.11 – High pressure equilibrium cell of the VLE Apparatus #2.....   | 47 |
| Figure A. 1 – Calibration certificate of the PT100 from apparatus #1  | 84 |
| Figure A. 2 – Calibration certificate of the pressure transducer with lower range (0-0.4MPa) .  | 85 |
| Figure A. 3 – Calibration certificate of the pressure transducer with higher range (0-1.7MPa)   | 86 |
| Figure A. 4 – Calibration certificate of the PT100 from apparatus #2 .....  | 87 |

# Table Index

---

|  | <b>Page</b> |
|--|-------------|
| Table 2.1 – Modifications to the Attractive Term of van der Waals Equation.....  | 15          |
| Table 2.2 – Modifications to the Attractive Term of van der Waals Equation.....  | 16          |
| Table A. 1 – Parameters for the polynomial equations of molar fraction vs density for water+ethanol                            | 88          |
| Table A. 2 – Parameters for the polynomial equations of molar fraction vs density for water+1-propanol .....                   | 89          |
| Table A. 3 – Parameters for the polynomial equation of molar fraction vs density for ethanol+1-propanol .....                  | 89          |
| Table A. 4– Stability of the air bath at 296,55K with or without ventilation and with or without filling with steel mesh ..... | 90          |
| Table A. 5- Stability of the air bath at 423.15K with or without filling with steel mesh .....                                 | 90          |

# Notation

---

## **Abbreviations**

|            |   |
|------------|---|
| An         | Analytical method   |
| AnGrav     | Gravimetric Analytical method                             |
| AnP        | Isobaric Analytical method                                |
| AnPT       | Isobaric-Isothermal Analytical method                     |
| AnT        | Isothermal Analytical method                              |
| AnSpec     | Spectroscopic Analytical method                           |
| AnOth      | Other Analytical method                                   |
| ADD y      | average absolute deviation of vapour phase molar fraction |
| AARD p     | average absolute relative deviation of pressure           |
| ASSOC      | association   |
| CHAIN      | chains  |
| CSRK       | Carnahan-Starling Redlich-Kwong                           |
| ELV        | equilibrio líquido vapour                                 |
| EOS        | Equation of State   |
| GC         | Gas Chromatography  |
| MONO       | monomeric   |
| NRTL       | Non-Random Two Liquid model                               |
| OD         | outside diameter  |
| PR         | Peng-Robinson   |
| PT         | Platinum Thermometer                                      |
| <i>PVT</i> | pressure volume temperature                               |
| RTD        | resistance temperature detectors                          |
| RK         | Redlich-Kwong   |
| SAFT       | statistical associating fluid theory                      |
| SAFT-VR    | statistical associating fluid theory - variable range     |
| SRK        | Soave-Redlich-Kwong                                       |
| Syn        | Synthetic method  |
| SynNon     | Non-Visual Synthetic method                               |

|         |  |
|---------|--|
| SynOth  | Other Synthetic method                         |
| SynP    | Isobaric Synthetic method                      |
| SynT    | Isothermal Synthetic method                    |
| SynVis  | Visual Synthetic method                        |
| UNIQUAC | UNIversal QUAsiChemical                        |
| UNIFAC  | UNIQUAC Functional-group Activity Coefficients |
| VLE     | vapour liquid equilibrium                      |
| Att     | attractive                                     |

### **Latin Alphabet**

|         |  |
|---------|--|
| $a$     | equation of state parameter  |
| $a_i$   | activity of the component $i$  |
| $a(T)$  | equation of state temperature dependent term                             |
| $A$     | Helmholtz function   |
| $A^l$   | ideal Helmholtz function   |
| $A^r$   | residual Helmholtz function  |
| $b$     | equation of state parameter  |
| $c$     | equation of state parameter  |
| $d$     | equation of state parameter  |
| $e$     | equation of state constant   |
| $f_i$   | fugacity of component $i$  |
| $f_i^0$ | standard-state fugacity  |
| $k$     | Boltzmann constant; equation of state constant                           |
| $l$     | liquid   |
| $m$     | number of segments; number of monomers                                   |
| $n_i$   | number of moles of components $i$  |
| $p$     | pressure   |
| $p_c$   | critical pressure  |
| $R$     | Universal gas constant; $1/4\pi$ multiple of the mean curvature integral |
| $T$     | temperature  |
| $T_c$   | critical temperature   |
| $u$     | equation of state parameter  |



|       |                                    |
|-------|------------------------------------|
| $V$   | volume                             |
| $v$   | vapour                             |
| $w$   | equation of state parameter        |
| $x$   | molar fraction in the liquid phase |
| $y$   | molar fraction in the vapour phase |
| $Z$   | compressibility factor             |
| $Z_c$ | critical compressibility factor    |

### ***Greek Alphabet***

|               |   |
|---------------|---|
| $\alpha$      | non-sphericity parameter                                  |
| $\beta$       | equation of state parameter                               |
| $\varepsilon$ | energy of interaction; depth parameter of attractive well |
| $\phi_i^V$    | fugacity coefficient of the vapour phase                  |
| $\phi_i^L$    | fugacity coefficient of the liquid phase                  |
| $\gamma$      | Activity coefficient                                      |
| $\eta$        | packing fraction  |
| $\lambda$     | equation of state parameter, width of well                |
| $\mu$         | chemical potential  |
| $\xi$         | interaction parameter                                     |
| $\rho$        | number density  |
| $\sigma$      | distance of interaction between molecules                 |
| $\omega$      | acentric factor   |

# Chapter 1 - Introduction

For many chemical products (especially commodity chemicals), the cost of separation makes a significant contribution to the total cost of production. In fact, there is a strong economic incentive to perform separations with optimum efficiency. However the rational design of a typical separation process (for example, distillation), we need the thermodynamic properties of mixtures. In particular, for a system that has two or more phases at some temperature and pressure, the equilibrium concentrations of all components in all phases are required. This makes Thermodynamics the most important tool towards the optimization of one of the cornerstones of chemical engineering that is the separation of fluid mixtures [1].

There are many ways to obtain information about the phase behavior of fluid mixtures, but the direct measurement of phase-equilibrium remains an important source of information, though it is difficult and expensive to obtain accurate experimental data [2]. Even when applied thermodynamics is used to calculate the phase behavior of a mixture, experimental data are important, because in this case, it is primarily a tool for analyzing the robustness of the experimental data. However, without some experimental information, this “stretching” cannot generate anything useful. In fact, at least some experimental data points are needed to adjust interaction parameters [1-3]. Therefore, for a progress in applied thermodynamics, the role of experiments is essential [1].

Useful compilations of high-pressure fluid-phase-equilibria data have been done over the years by some authors. These compilations have proven to be helpful in a much faster way to seek experimental results for comparison. This compilation divides the results per binary, ternary or multicomponent mixtures and by the type of method used (see chapter 3). Knapp *et al.* [4] presented the compiled data covering the period 1900–1980. After these authors, others followed. Fornari *et al.* [5] covered 1978–1987, Dohrn and Brunner [6] 1988–1993, Christov and Dohrn [7]

1994–1999, Dohrn *et al.* [1] 2000-2004 and more recently Fonseca *et al.* [8] 2005-2008. In all of these papers we have found that the binary mixtures of water+alcohol or even the binary mixtures of primary alcohols have few results providing enforcement for acquiring such data. This work will contribute to increase the number of data in that area and complement the existing ones.

## 1.1. Objectives

This PhD project, included in the Technological Chemistry area, has the aim to provide the community with accurate VLE data at high temperatures for water+alcohols and alcohols+alcohols binary mixtures, to facilitate efficient high temperature separation of these compounds through high temperature distillation. The implementation of this thesis involves the following specific objectives:

1. Upgrading the existing VLE flow apparatus, by improving the temperature control of the equilibrium cell and pressure transducers accuracy, for ethanol-water measurements up to 423.2K.
2. Constructing a new VLE flow apparatus, including a new oven with a better temperature control and capable of reaching temperatures up to 573.2K and pressures up to 20 MPa.
3. VLE measurements, in the temperature range 373.2 to 423.2K, for several binary compositions of systems:
  - Ethanol – water;
  - 1-propanol – water;
  - Ethanol+1-propanol.
4. Modeling the VLE measurements using the Statistical Associating Fluid Theory for potentials of Variable Range (SAFT-VR) equation of state.

## **1.2. Outline of thesis**

In chapter 1 an introduction is made presenting the main objectives and the outline of this thesis.

In Chapter 2, a brief review of Vapour-Liquid Equilibria (VLE) is given. Hundreds of equations representing the *PVT* behaviour of fluids have been proposed, few before van der Waals, but mostly later. They have a central role in the thermodynamics of fluids. In this chapter a review of these theoretical methods of VLE property prediction is discussed as an introduction to the equation used to model the experimental results, the Statistical Associating Fluid Theory for potentials of Variable Range (SAFT-VR).

In Chapter 3 we give a detailed description of the classification of VLE Experimental Methods, as a support and justification to our chapter 4, in which a description of the chosen apparatus is made, as well as the experimental procedure. The description of the new apparatus (under construction) is also made.

Chapter 5 presents the results and discussion in the article form. Paper I refers to the evaluation of performance of the VLE apparatus using water and water-ethanol system as their behaviour has been extensively studied and accurate data is available for comparison. New data have been obtained for temperatures between 363.3 and 423.7 K, and pressures up to 1 MPa. Paper II refers to the results of VLE measurements for the systems water-1-propanol, and Paper III the measurements for the ethanol+1-propanol binary mixture. In all of these papers a correlation with the SAFT-VR equation was carried out. These studies show that the phase equilibria is accurately described with this model.

In Chapter 6 of this thesis, we will give the final conclusions and overall comments of our work and an outlook on the possible future research in related subjects.

### **1.3. Bibliography**

- [1]. J.M. Prausnitz and F.W. Tavares, *Thermodynamics*, 50 (2004) 739-761
- [2]. R. Dohrn, S. Peper and J. Fonseca, *Fluid Phase Equilibria*, 288 (2010) 1-54
- [3]. P. Uusi-Kyyny, Juha-Pekka Pokki, M. Laakkonen, J. Aittamaa and S. Liukkonen, *Fluid Phase Equilibria*, 201 (2002) 343-358
- [4]. H. Knapp, R. Döring, L. Oellrich, U. Plöcker, J. M. Prausnitz, *DECHEMA Chem. Data Series VI*, Frankfurt (1981)
- [5]. R.E. Fornari, P. Alessi and I. Kikic, *Fluid Phase Equilibria*, 57 (1990) 1-33
- [6]. R. Dohrn and G. Brunner, *Fluid Phase Equilibria*, 106 (1995) 213-282
- [7]. M. Christov and R. Dohrn, *Fluid Phase Equilibria*, 202 (2002) 153-218
- [8]. J.M.S. Fonseca, R. Dohrn and S. Peper, *Fluid Phase Equilibria*, 300, (2011) 1-69

# Chapter 2 - Vapour-Liquid Equilibrium Modeling

## 2.1. Introduction

The scientific literature on fluid phase equilibria goes back well over 150 years and has reached enormous proportions, including thousands of articles and hundreds of books and monographs.

In the chemical process industries, fluid mixtures are often separated into their components by operations, such as distillation, absorption, and extraction. The design of such operations requires quantitative estimates of the partial equilibrium properties of fluid mixtures. Whenever possible, such estimates should be based on reliable experimental data for the particular mixture at conditions of temperature, pressure, and composition.

Unfortunately, such data are often not available. In typical cases, only fragmentary data are available and it is then necessary to reduce and correlate the limited data to make the best possible interpolations and extrapolations. One example is the study of the fluid-phase behavior of water-linear alcohols binary mixtures. Despite the various studies of properties of these pure fluids, there is a lack of data at high pressures and temperatures [1]. Phase equilibrium measurements are both difficult and expensive, and it is necessary to maximize the information and understand for a particular system what can be obtained from a minimum amount of experimentation. The costs of vapour liquid equilibria data vary with the type of equipment and system studied and the number of experiments. If we take into account the equipment development, the costs are very high.

For systems of more than two components, the experimental work necessary to obtain a complete phase diagram reaches impractical requirements. For this and others reasons the use of VLE computational modelling has grown. In this chapter we talk briefly about the thermodynamics of the vapour-liquid equilibria, the evolution of the equations of state and the types of experimental methods for obtaining vapour-liquid equilibria data.

## 2.2. Thermodynamics of Vapour - Liquid Equilibrium (VLE)

In thermodynamics the term “vapour-liquid equilibrium” refers to systems with liquid and vapour phases in equilibrium. Here we consider a system in which a single liquid phase is in equilibrium with its vapour phase at a given temperature and pressure. In terms of Gibbs language we say that for every component  $i$  in the mixture, the condition of thermodynamic equilibrium is given by

$$f_i^V = f_i^L \quad \text{equation 2.1}$$

where  $f_i$  is the fugacity of component  $i$ ,  $V$  for vapour and  $L$  for liquid [1]. To fully understand the equilibrium we need to quantify the quantities of interest that are the temperature, the pressure, and the compositions of both phases. Given some of these quantities, our task is to calculate the others. The fundamental problem is to relate these fugacities with the mixture composition in both phases, because the fugacity of a component in a mixture depends on the temperature, pressure, and composition of the mixture.

Two different strategies can be used to calculate the fugacities in both phases. In the first one we relate  $f_i^V$  and  $f_i^L$  to temperature, pressure, and mole fraction, introducing the vapour-phase and liquid phase fugacity coefficients  $\phi_i^V$  and  $\phi_i^L$

$$\phi_i^V = \frac{f_i^V}{y_i P} \quad \text{equation 2.2}$$

$$\phi_i^L = \frac{f_i^L}{x_i P} \quad \text{equation 2.3}$$

where  $y_i$  is the vapour phase and  $x_i$  is the liquid phase molar fractions. The fugacity coefficients can be calculated from vapour phase  $PVT$   $y$  data, usually given by an equation of state [1].

Deviations from ideal behavior are more likely to occur in the liquid phase than in the vapour phase. As a result of smaller intermolecular distances, the forces of interaction between molecules in the liquid are considerably stronger. In contrast, the vapour phase can be assumed to behave ideally from low to moderate pressures. At higher pressures, the fugacity coefficients for the vapour phase must be calculated using an equation of state [2].

In the first strategy the calculations use equation 2.2 to determine  $f_i^v$ , while for the liquid phase the fugacity of the component  $i$  by the equation 2.3. Furthermore, the fugacity coefficients of the components in both phases can be calculated using the relation:

$$\ln \phi_i = \int_V^\infty \left[ \frac{1}{RT} \left( \frac{\partial P}{\partial n_i} \right)_{T,V,n_{j \neq i}} - \frac{1}{V} \right] dV - \ln Z \quad \text{equation 2.4}$$

where  $Z$  is the compressibility factor,  $pV/RT$ . This relation is very useful for cubic equations of state.

In the second strategy the phase behavior of real liquids is usually described by using the activity coefficient concept  $\gamma_i$  :

$$\gamma_i \equiv \frac{a_i}{x_i} = \frac{f_i^L}{x_i f_i^0} \quad \text{equation 2.5}$$

where  $a_i$  is the activity of the component  $i$ , and  $f_i^0$  the fugacity of pure liquid at the same temperature and pressure of the mixture (standard-state fugacity). In this case the calculus is based on activity coefficient models, such as Margules, Van Laar, Wilson, NRTL, UNIFAC and UNIQUAC in which we calculate phase equilibrium compositions from excess Gibbs energy [2].

The use of the first strategy for mixture calculations needs information on pure components and like and unlike binary interactions. On the other hand, this



approach requires no standard states for the components in the mixtures, in contrast with the second strategy. These advantages are especially important for mixtures containing supercritical components.

The main disadvantage of the second strategy is the problem of the non-existence of accurate equation of state, which describes complex liquids, like associated fluids with hydrogen bonding. Due to these advantages of the first strategy, it was chosen for the current work.

In the next subchapter we will introduce the equation of state used in this work, presenting a review about the evolution of the equations of state, namely the cubic ones, which have been used in many engineering calculations.

### **2.3. Modelling Vapour - Liquid Equilibrium with Equations of State (EOS)**

Equations of state play an important role in chemical engineering design and they have assumed an expanding role in the study of the phase equilibria of fluids and fluid mixtures [3]. In view of the variety of chemical species and applications, it is not astonishing that until today hundreds of equations of state have been published; if variants are counted, too, the total exceeds thousands. It happens frequently that authors of new equations of state, or of new variants of existing equations of state, report significant improvements with regard to properties and substances they are interested in, but fail to comment on the applicability or consequences beyond their own immediate field of research. The readers of such a publication sometimes have difficulties to access its importance or applicability to their own problems. Furthermore, some sub-functions or terms of equations of state are known to be more efficient than others for describing real fluids, especially if wide ranges of temperatures and pressures are concerned. There is now a considerable expertise available on the relation between functional forms of equations of state and their capability to correlate various thermodynamic properties; unfortunately, this information is not always taken into account [4].

Generally, equations of state can be distinguished mainly in empirical, theoretical and semi-empirical (or semi-theoretical) equations. Comprehensive reviews can be found in the works of many authors [5-10].

Empirical equations usually need a large amount of experimental data of pure components and contain a large number of substance-specific parameters with little physical meaning. Their application is restricted to a very limited number of substances or just one component and their lack of predictive power beyond the pressure–temperature limit where they have been developed makes them impractical for general purposes [11].

Theoretical equations are based on statistical thermodynamic insight. They have fewer substance-dependent parameters, and these parameters have physical meaning. They require time-consuming calculations and suffer from limitations of existing theories, making their predictions less accurate. However, they may represent property trends correctly even far away from their fitting range. For instance, the well-known Virial Equation of State may be regarded as an empirical equation i.e., as a power series in density, with coefficients to be fitted to experimental data, as well as, a theoretical equation if the coefficients are calculated from the appropriate integrals over Boltzmann factors [4,11].

Semi-empirical EOSs combine features of both theoretical and empirical equations, for example, they provide good results for a large number of pure components and their predictions beyond the pressure–temperature limit of the experimental data used to develop them are often acceptable. Due to these facts this is the most extensively used type of EOS for prediction of phase equilibrium and thermodynamic properties of fluids. Moreover, semi-empirical EOSs offer the fastest way to make quantitative predictions of thermophysical properties of pure substances and mixtures with few experimental determinations using few adjustable parameters [11].

### 2.3.1. From Van der Waals to SAFT

Many equations of state have been proposed in the literature over the years with either an empirical, semi-empirical or theoretical basis. It would take a very long thesis to describe all of them, their weaknesses, their strengths and their limitations. Some are better for volumes, others for phase equilibria, but they all have something in common: their beginning.

The history of the equation of state dates back to at least 1662 when Boyle conducted his experiments on air and deduced that, at a given temperature, the volume of a fixed mass of gas is inversely proportional to its pressure ( $PV=\text{constant}$ ). The effect of temperature was observed by Charles in 1787 and later by Gay-Lussac who, in 1802, found the dependence of volume on temperature to be linear at constant pressure. Together with Dalton's law of partial pressures, postulated in 1801, these observations suggest the relation

$$P = \left(\sum_i n_i\right)RT / V \quad \text{equation 2.6}$$

that we recognize nowadays as the equation of state of a perfect gas mixture. After this breakthrough, the work of Faraday (1823), Andrews (1869) and others succeed and paved the way towards the modern view of an equation of state presented by van der Waals [12].

The van der Waals equation was the first equation to predict vapour-liquid coexistence over a century ago.

The history of this equation began in 1873, when van der Waals obtained his doctor's degree for a thesis entitled "*Over de Continuïteit van den Gas- en Vloeistofoestand*" (on the continuity of the gas and liquid state – Figure 2.1), which put him in the foremost rank of physicists. In this thesis, he proposed an "Equation of State" embracing both the gaseous and liquid state.

He demonstrated that the two states of aggregation not only merge into each other in a continuous manner, but that they were in fact of the same nature. This equation of state was a dramatic improvement over the ideal gas law. It was van der Waals' genius that made him see the necessity of taking into account the volumes of

molecules and the intermolecular forces ("van der Waals forces", as they are now generally called) in establishing the relationship between the pressure, volume, and temperature of gases and liquids. Van der Waals won the Nobel Prize for this work in 1910 [13].

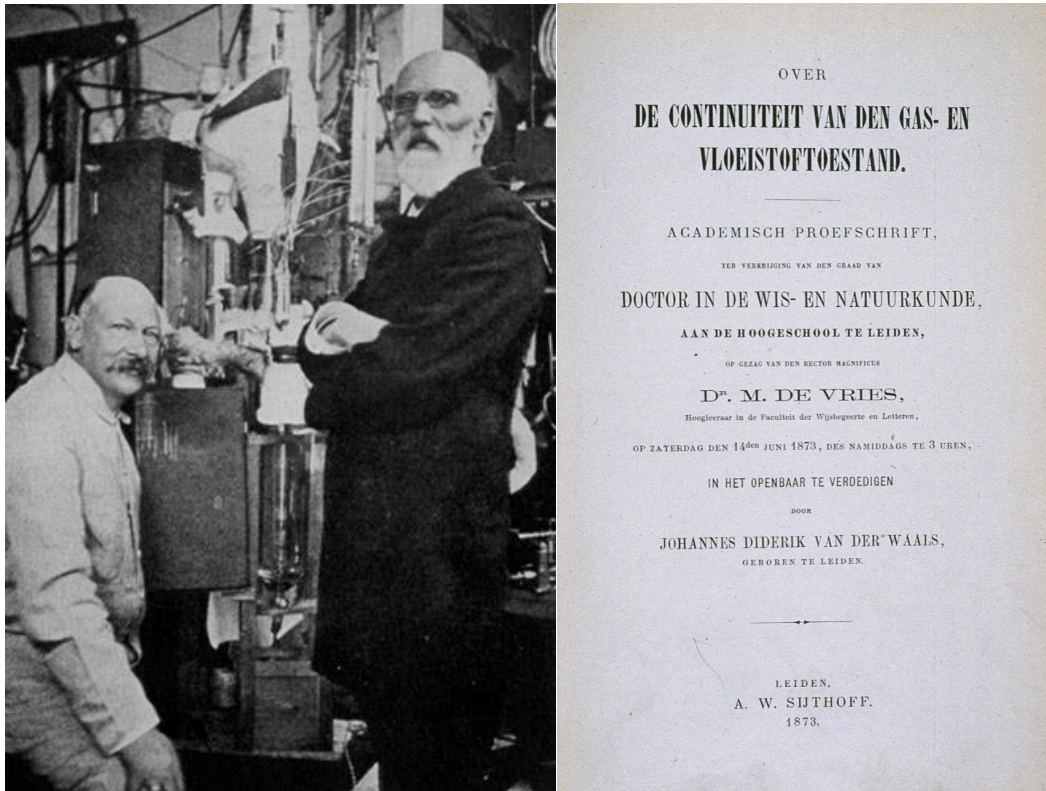


Figure 2.1 – Heike Kamerlingh Onnes (left) and van der Waals (right) in front of the helium-‘liquefactor’, Leiden 1908 [13]

**Error! Reference source not found.**7 gives us the van der Waals equation

$$Z = \frac{pV}{RT} = \frac{V}{V-b} - \frac{a}{RTV} \quad \text{equation 2.7}$$

where  $Z$  is the compressibility factor,  $T$  the temperature,  $V$  the volume,  $p$  the pressure and  $R$  the molar universal gas constant.

In this equation the parameter  $b$  gives us the co-volume occupied by molecules (repulsive part), whereas the parameter  $a$  gives us the attractive forces between molecules (attractive part).

From the beginning van der Waals knew that his “constant”  $b$  was not, in fact, a constant but a decreasing function of the density. So it was clear to him that one

should only use the equation with caution in  $P, V, T$  regions remote from those in which  $a$  and  $b$  had been determined. Nevertheless for many years, when his equation became well known, many physicists used it assuming  $a$  and  $b$  as true constants, ignoring the reservations set out by van der Waals. Then the attempt to invent new equations started, some intended for special applications, others purely empirical and some based on theoretical arguments [14]. Van der Waals devoted much effort in trying to discover the dependence of his parameters with temperature and density<sup>1</sup>. And because the application of the equation to the liquid state didn't provide with correction the properties of the state, many efforts were made by authors in improving the above equation, replacing the repulsive part by a more convenient expression and modifying the attractive term.

In Tables 2.1 and 2.2 from we can view some of the modifications to these terms. Perhaps, the most important model for the modification of the van der Waals equation of state is the Redlich-Kwong equation [16]. It retains the original van der Waals hard-sphere term with the addition of a temperature- dependent attractive term (equations 2.8 to 2.10) [3]:

$$Z = \frac{pV}{RT} = \frac{V}{V-b} - \frac{a}{RT^{1.5}(V+b)} \quad \text{equation 2.8}$$

$$a = 0.4278R^2T_c^{2.5} / p_c \quad \text{equation 2.9}$$

$$b = 0.0867RT_c / p_c \quad \text{equation 2.10}$$

where the subscript  $c$  indicates properties at the critical point. The success of the Redlich-Kwong equation has been the impetus for many further empirical improvements. More than 100 modifications to this equation have been proposed [12]. Soave in 1972 [17] suggested replacing the term  $a/T^{1.5}$  with a more general temperature-dependent term  $a(T)$  that is

$$Z = \frac{V}{V-b} - \frac{a(T)}{RT(V+b)} \quad \text{equation 2.11}$$

---

<sup>1</sup> "For a long time I searched for a definite characteristic to find whether just making  $b$  variable is sufficient to bring about complete agreement between my formula and experiment, ..., whether perhaps it is necessary to assume variability of  $a$  and  $b$  with temperature..." van der Waals in his Nobel Prize acceptance text [15].

$$a(T) = 0.4274 \left( \frac{R^2 T_c^2}{p_c} \right) \left\{ 1 + m \left[ 1 - \left( \frac{T}{T_c} \right)^{0.5} \right] \right\}^2 \quad \text{equation 2.12}$$

$$m = 0.480 + 1.57\omega - 0.176\omega^2 \quad \text{equation 2.13}$$

$$b = 0.08664RT_c / p_c \quad \text{equation 2.14}$$

where  $\omega$  is the acentric factor, proposed by Pitzer in 1955 [18].

To test the accuracy of Soave-Redlich-Kwong (SRK) equation, the vapour pressure of a number of hydrocarbons and several binary systems were calculated and compared with experimental data. In contrast to the original Redlich-Kwong equation, Soave's modification fitted the experimental curve well and was able to predict the phase behavior of mixtures in the critical region, and today is one of the most used equations together with the Peng-Robinson equation of state [3].

In 1976, Peng and Robinson [18] redefined  $a(T)$  as:

$$a(T) = 0.45724 \left( \frac{R^2 T_c^2}{p_c} \right) \left\{ 1 + k \left[ 1 - \left( \frac{T}{T_c} \right)^{0.5} \right] \right\}^2 \quad \text{equation 2.15}$$

$$k = 0.37464 + 1.5422\omega - 0.26922\omega^2 \quad \text{equation 2.16}$$

$$b = 0.07780RT_c / p_c \quad \text{equation 2.17}$$

Recognizing that the critical compressibility factor of the Redlich-Kwong equation is overestimated, they also proposed a different volume dependence.

$$Z = \frac{pV}{RT} = \frac{V}{V-b} - \frac{a(T)}{RT[V(V+b) + b(V-b)]} \quad \text{equation 2.18}$$

The Peng-Robinson equation of state (PR) slightly improves the prediction of liquid volumes and predicts a critical compressibility factor of  $Z_c=0.307$ . Peng and Robinson [19] gave examples of the use of their equation for predicting the vapour pressure and volumetric behavior of single-component systems, and the phase behavior and volumetric behavior of the binary, ternary, and multicomponent

system and concluded that the equation can be used to accurately predict the vapour pressures of pure substances and equilibrium ratios of mixtures. The Peng-Robinson equation performed as well as Soave-Redlich-Kwong equation [3].

The Peng-Robinson and Soave-Redlich-Kwong equations are used widely in industry. The advantages of these equations are that they can accurately and easily represent the relation among temperature, pressure, and phase compositions in binary and multicomponent systems. They only require the critical properties and acentric factor for the generalized parameters. Little computer time is required and good phase equilibrium correlations can be obtained. However, the success of these modifications is restricted to the estimation of vapour pressure. The calculated saturated liquid volumes are not improved and are invariably higher than experimental measurements [3]. In Table 2.2 a summary of the most important modifications to the attractive term of the van der Waals equation is presented where these equations are represented.

Table 2.1 – Modifications to the Attractive Term of van der Waals Equation

| Equation                               | Attractive Term ( $-Z^{att}$ )           |
|--|--|
| <b>Redlich-Kwong (RK) [16]</b>         | $\frac{a}{RT^{1.5}(V+b)}$                |
| <b>Soave (SRK) [17]</b>                | $\frac{a(T)}{RT(V+b)}$                   |
| <b>Peng-Robinson (PR) [19]</b>         | $\frac{a(T)V}{RT[V(V+b)+b(V-b)]}$        |
| <b>Fuller [20]</b>                     | $\frac{a(T)}{RT(V+cb)}$                  |
| <b>Heyen [10]</b>                      | $\frac{a(T)V}{RT[V^2+(b(T)+c)V-b(T)c]}$  |
| <b>Schmidt-Wenzel [21]</b>             | $\frac{a(T)V}{RT(V^2+ubV+wb^2)}$         |
| <b>Hermens-Knapp [22]</b>              | $\frac{a(T)V}{RT[V^2+Vcb-(c-1)b^2]}$     |
| <b>Kubic [23]</b>                      | $\frac{a(T)V}{RT(V+c)^2}$                |
| <b>Patel-Teja (PT) [24]</b>            | $\frac{a(T)V}{RT[V(V+b)+c(V-b)]}$        |
| <b>Adachi <i>et al.</i> [25]</b>       | $\frac{a(T)V}{RT[(V+b_2)(V+b_3)]}$       |
| <b>Strjek-Vera (SV) [26]</b>           | $\frac{a(T)V}{RT[(V^2+2bV-b^2)]}$        |
| <b>Yu and Lu [27]</b>                  | $\frac{a(T)V}{RT[V(V+c)+b(3V+c)]}$       |
| <b>Treble and Bishnol (TB) [28]</b>    | $\frac{a(T)V}{RT[(V^2+(b+c)V-(bc+d^2)]}$ |
| <b>Schwartzentruber and Renon [29]</b> | $\frac{a(T)V}{RT[(V+c)(V+2c+b)]}$        |



The other way to modify the van der Waals equation is to examine the repulsive term of a hard-sphere fluid (Table 2.2). Many accurate representations have been developed theoretically and by computer simulation for the repulsive interactions of hard spheres and incorporated into an equation of state, for example in the work of Carnahan and Starling [30] and Guggenheim [31]. Perhaps the most widely used alternative to the van der Waals hard-sphere term is the equation proposed by Carnahan and Starling :

$$Z = \frac{1 + \eta + \eta^2 - \eta^3}{(1 - \eta)^3} \quad \text{equation 2.19}$$

where  $\eta = b/4V$ .

**Table 2.2 - Modifications to the Attractive Term of van der Waals Equation**

| Equation                          | Repulsive Term ( $Z^{hs}$ )   |
|-----------------------------------|---|
| <b>Reis set al. [32]</b>          | $\frac{1 + \eta + \eta^2}{(1 - \eta)^3}$  |
| <b>Thiele [33]</b>                | $\frac{1 + \eta + \eta^2}{(1 - \eta)^3}$  |
| <b>Guggenheim [32]</b>            | $\frac{1}{(1 - \eta)^4}$  |
| <b>Carnahan and Starling [31]</b> | $\frac{1 + \eta + \eta^2 - \eta^3}{(1 - \eta)^3}$   |
| <b>Scott et al. [34]</b>          | $\frac{RT(V + b)}{V(V - b)}$  |
| <b>Boublik [35]</b>               | $\frac{1 + (3\alpha - 2)\eta + (3\alpha^2 - 3\alpha + 1)\eta^2 - \alpha^2\eta^3}{(1 - \eta)^3}$ |

Other equations of state have been formed by modifying both attractive and repulsive terms, or by combining an accurate hard-sphere model with an empirical temperature dependent attractive contribution. Carnahan and Starling [36] combined the Redlich-Kwong attractive term with their repulsive term - CSRK

$$Z = \frac{1 + \eta + \eta^2 - \eta^3}{(1 - \eta)^3} - \frac{a}{RT^{1.5}(V + b)} \quad \text{equation 2.20}$$

This equation is one of the most known equations that modifies both attractive and repulsive terms.

For many decades these methods for describing the thermodynamic behavior of fluids composed of simple molecules were effective. By simple, we mean molecules for which the most important intermolecular forces are repulsion and dispersion (van der Waals attractions). Many hydrocarbons, natural gas constituents, simple organic molecules (e.g., methyl chloride, toluene), and simple inorganics (N<sub>2</sub>, CO, O<sub>2</sub>, N<sub>2</sub>O, etc.) fall within this category.

Nevertheless, many fluids, and particularly mixtures, do not fall within this simple class, like polar solvents, hydrogen-bonded fluids, and so on. The correlation of data requires complex and unphysical mixing rules and temperature dependent binary parameters, and the predictive capability of the approach is usually very poor. The reason for this is that, for such fluids, important new intermolecular forces come into play [37].

The first mixing rules were proposed by Zudkevitch and Joffe [38] for the Redlich Kwong equation of state:

$$\begin{aligned}
 a &= \sum_{i < j} x_i x_j a_{ij} \\
 b &= \sum_i x_i b_i \\
 a_{ij} &= \left(1 - k_{ij}\right) \left(a_i a_j\right)^{1/2}
 \end{aligned}
 \tag{equations 2.21}$$

An important class of these complex fluids consists of those that associate to form relatively long-lived dimers or higher *n*-mers. This class of fluids includes those in which hydrogen bonding, charge transfer, and other types of complex interactions can occur, for example linear alcohols. So they require special treatment when being modeled.

A more promising route for understanding the properties of these associating fluids is provided by recent theories that are firmly based in statistical mechanics. In principle, statistical mechanics provides formal recipes for calculating the structure and thermodynamics of a fluid given its intermolecular potential function. However, for most systems of interest, this solution requires the use of one or more

approximations that ultimately determine the accuracy of the theory [37]. The next section explains one of these new routes as it introduces one equation of state that has grown in the past decade the Statistical Associating Fluid Theory, abbreviated as SAFT.

### 2.3.2. SAFT EOS

In 1990, Chapman *et al.* [39-40] proposed an approach capable of determining the properties of the liquid and vapour phase. This model called Statistical Associating Fluid Theory, normally called SAFT, was developed from the Wertheim's theory [41-46].

Within the framework of SAFT, the EOS of a fluid is a perturbation expansion given in terms of the residual molar Helmholtz energy  $A^r$ , defined as the difference between the total molar Helmholtz energy and that of an ideal gas at the same temperature  $T$  and molar density  $\rho$ :

$$A^r(T, \rho) = A(T, \rho) - A^{IDEAL}(T, \rho) \quad \text{equation 2.22}$$

SAFT implicitly assumes that there are three major contributions to the total intermolecular potential of a given molecule:

- the repulsion-dispersion contribution typical of individual segments,
- the contribution due to the fact that these segments can form a chain,
- the contribution due to the possibility that some segments form association complexes with other molecules.

The residual Helmholtz energy is given within the SAFT formalism (equation 2.23) as a sum of the contributions from these different intermolecular effects

$$A^r = A^{MONO} + A^{CHAIN} + A^{ASSOC} \quad \text{equation 2.23}$$

where the superscripts *MONO*, *CHAIN*, and *ASSOC* refer to the contributions from the "monomeric" segments, from the formation of chains, and from the existence of association sites, respectively.

By combining the above equations we obtain the usual forms of the SAFT equation:

$$A = A^{IDEAL} + A^{MONO} + A^{CHAIN} + A^{ASSOC} \quad \text{equation 2.24}$$

$$\frac{A}{NkT} = \frac{A^{IDEAL}}{NkT} + \frac{A^{MONO}}{NkT} + \frac{A^{CHAIN}}{NkT} + \frac{A^{ASSOC}}{NkT} \quad \text{equation 2.25}$$

where  $N$  is the number of molecules,  $k$  the Boltzmann constant, and  $T$  the absolute temperature.

Hence, a SAFT fluid is a collection of monomers that can form covalent bonds; the monomers can interact via repulsive and attractive (dispersion) forces and, in some cases, association interactions. The many different versions of SAFT essentially correspond to different choices for the monomer fluid and different theoretical approaches to the calculation of the monomer free energy and structure. Perhaps the most popular are the Perturbed-Chain and Variable Range versions of the SAFT approach (PC-SAFT and SAFT-VR, respectively) [47]. In the next section we give a brief overview on the model used to correlate our data, the SAFT-VR model.

#### *SAFT-VR Model*

In the approach of Mac Dowell *et al.* [48], water is represented as a single spherical segment ( $m = 1$ ) with four associating sites, two representing the hydrogen atoms and two the lone electron pairs. For ethanol and 1-propanol one association site representing the hydroxyl hydrogen atom and two the oxygen lone electron pairs are included; in this case, the number of spherical segments is 1.533 accounting for the elongated molecular shape (Figure 2.2). It should be noted that, both in the pure compounds and in the mixture, the associative interactions are only allowed between sites of different type, namely “hydrogen-type” sites can only interact with “electron-type” sites and vice versa.

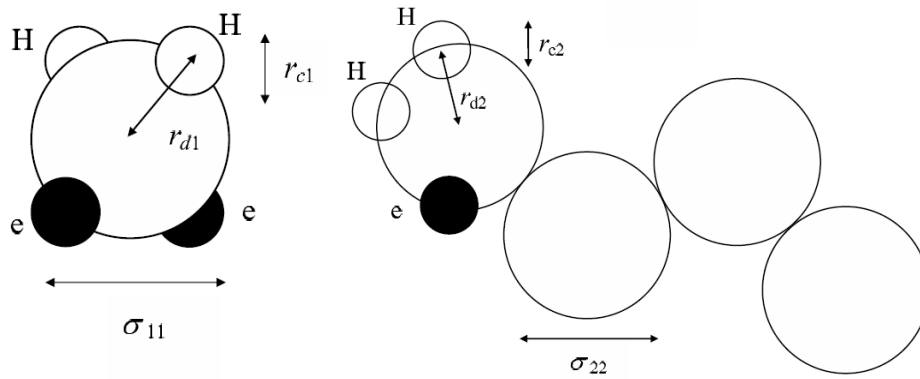


Figure 2.2 - SAFT-VR model for water (on the left) and alcohol (on the right)

The inter and intramolecular cross interactions between segments are obtained from the modified Lorentz-Berthelot combining rules [49]:

$$\sigma_{ij} = \frac{\sigma_{ii} + \sigma_{jj}}{2} \quad \text{equation 2.26}$$

$$\varepsilon_{ij} = (1 - k_{ij}) \sqrt{\varepsilon_{ii} \varepsilon_{jj}} \quad \text{equation 2.27}$$

$$\lambda_{ij} = \gamma_{ij} \frac{\sigma_{ii} \lambda_{ii} + \sigma_{jj} \lambda_{jj}}{\sigma_{ii} + \sigma_{jj}} \quad \text{equation 2.28}$$

Being SAFT-VR a new model when compared to those that are traditional in Chemical Engineering, the data available for the use of this type of correlation with binary mixtures of water+alcohol and alcohol+alcohol is limited. However, in more than 20 years, there has been an increase in the amount of papers using this type of equation to correlate experimental data. For full details of the SAFT-VR expressions the reader is directed to the original paper [50].

## 2.4. Bibliography

- [1]. Bruce E. Poling, J.M. Prausnitz and J.P. O'Connell, The Properties of Gases and Liquids, McGraw-Hill Book Co. Singapore, 2001
- [2]. M.B. Mane and S.N. Shinde, Sci. Revs. Chem. Commun. 2 (2012) 158-171
- [3]. Y.S. Wei and R.J. Sadus, AIChE Journal 46 (2000) 169-196
- [4]. U. Deiters, Fluid Phase Equilibria 161 (1999) 205-219
- [5]. J.J. Martin, Ind. Eng. Chem. Fundam. 18 (1979) 81-97
- [6]. K.E. Gubbins, Fluid Phase Equilibria 13 (1983) 35-57

- [7]. C. Tsonopoulos and J.L. Heidman *Fluid Phase Equilibria* 24 (1985) 1-23
- [8]. S.J. Han, H.M. Lin and K.C. Chao, *Chem. Eng. Sci.* 43 (1988) 2327-2367
- [9]. A. Anderko, *Fluid Phase Equilibria* 61 (1990) 145-225
- [10]. S.I. Sandler, *Models for thermodynamic and phase equilibria calculations*, Marcel Dekker (1994) New York
- [11]. F. Abdollahi-Demneh, M.A. Moosavian, M.M. Montazer-Rahmati, M.R. Omidkhan and H. Bahmaniar, *Fluid Phase Equilibria* 288 (2010) 67-82
- [12]. M. Assael, J.P. Martin Trusler and T.F. Tsolakis, *Thermophysical Properties of Fluids, An Introduction to their Prediction*, Imperial College Press, London 1996
- [13]. [http://www.nobelprize.org/nobel\\_prizes/physics/laureates/1910/waals-bio.html](http://www.nobelprize.org/nobel_prizes/physics/laureates/1910/waals-bio.html)
- [14]. A.Y. Kipnis, B.E. Yavelov and J.S. Rowlinson, *Van der Waals and Molecular Science*, Clarendon Press, New York, 1996
- [15]. <http://www.scs.illinois.edu/~mainzv/exhibit/vanderwaals.htm>
- [16]. O. Redlich and J. N. S. Kwong, *Chem. Res.* 44 (1949) 233-244
- [17]. G. Soave, *Chem. Eng. Sci.* 27(1972) 1197-1203
- [18]. K. S. Pitzer, *J. Amer. Chem. Soc.* 77, (1955) 3433-3440
- [19]. D.Y. Peng and D. B. Robinson, *Ind. Eng. Chem. Fundam.* 15 (1976) 59-64
- [20]. G.G. Fuller, *Ind. Eng. Chem. Fundam.* 15 (1976) 254-257
- [21]. G. Schmidt and H. Wenzel, *Chem. Eng. Sci.* 35 (1980) 1503-1512
- [22]. A. Harmens and H. Knapp, *Ind. Eng. Chem. Fundam.* 19 (1980) 291-294
- [23]. W.L. Kubic, *Fluid Phase Equilib.* (1982) 9, 79-97
- [24]. N.C. Patel and A.S. Teja, *Chem. Eng. Sci.* 37 (1982) 463-473
- [25]. Y. Adachi, B.C. Lu and H. Sugie, *Fluid Phase Equilib.* 13 (1983) 133-142
- [26]. R. Stryjek and J.H. Vera, *Can. J. of Chem. Eng.*, 64 (1986) 323-333
- [27]. J.M. Yu and B.C. Lu, *Fluid Phase Equilib.* (1987) 34, 1-19
- [28]. M.A. Trebble and P.R. Bishnoi, *Fluid Phase Equilib.* 40 (1987) 1-21
- [29]. J. Schwartzentruber and H. Renon, *Fluid Phase Equilib.* 52 (1989) 127-134
- [30]. N.F. Carnahan and K. E. Starling, *J. Chem. Phys.* 51 (1969) 635-636
- [31]. E.A. Guggenheim, *Mol. Phys.*, 9 (1965) 199-200
- [32]. N.R. Reiss, H.L. Frisch and J.L.L. Lebowitz. *J. Chem. Phys.*, 31 (1959) 369-380
- [33]. E. Thiele, *J. Chem. Phys.* 39 (1963) 474-479

- [34]. R.L. Scott H. in Eyring, D. Henderson and W. Jost (Eds.), *Physical Chemistry, An Advanced Treatise*, vol. 8A: Liquid State. Academic press, New York, 1971
- [35]. T. Boublik, *Ber. Bunsenges. Phys. Chem.* 85 (1981)1038-1041
- [36]. N.F. Carnahan and K. E. Starling, *AIChE J.* 18 (1972) 1184-1189
- [37]. E.A. Müller and K.E. Gubbins, *Ind. Eng. Chem. Res.* 40 (2001) 2193-2211
- [38]. D. Zudkevitch and J. Joffe, *AIChE J.*, 16 (1970) 112-119
- [39]. W.G. Chapman, G. Jackson and K.E. Gubbins, *Mol. Phys.* 65 (1988) 1057-1079
- [40]. W.G. Chapman, K.E. Gubbins, G. Jackson and M. Radosz, *Ind. Eng. Chem. Res.* 29 (1990) 1709-1721
- [41]. M.S. Wertheim, *J. Stat. Phys.* 35 (1984) 19-34
- [42]. M.S. Wertheim, *J. Stat. Phys.* 35 (1984) 34-47
- [43]. M.S. Wertheim, *J. Stat. Phys.* 42 (1986) 459-476
- [44]. M.S. Wertheim, *J. Stat. Phys.* 42 (1986) 477-492
- [45]. M.S. Wertheim, *J. Chem. Phys.* 85 (1986) 2929-2936
- [46]. M.S. Wertheim, *J. Chem. Phys.* 87 (1987) 7323-7331
- [47]. H. Zhao, P. Morgado, A. Gil-Villegas and C. McCabe, *J. Phys. Chem. B*, 110 (2006) 24083-24092
- [48]. N. Mac Dowell, F. Llovel, C.S. Adjiman, G. Jackson, A. Galindo, *Ind. Eng. Chem. Res.* 49 (2010) 1883–1899
- [49]. Rowlinson, J. S., Swinton, F. L., *Liquids and Liquid Mixtures*, 3rd ed.; Butterworth Scientific, London, 1982
- [50]. A. Gil Villegas, A. Galindo, P.J. Whitehead, S.J. Mills, G. Jackson, A.N. Burgess, *J. Chem. Phys.* 106 (1997) 4168–4186

# Chapter 3 - VLE Experimental Methods

## 3.1. Introduction

High-pressure phase behavior is often complex and difficult to predict. At high pressures deviations from ideal behavior become much larger than at ambient or moderate pressures. Therefore, the experimental investigation is often the only suitable method to determine accurately the high-pressure phase behavior. Many different methods are used to measure high-pressure phase equilibria. The reason is that no single method is suitable to determine all different VLE behavior at different temperatures and pressures.

According to Nagahama [1] there are four different methods to measure high pressure phase equilibria:

1. Static method;
2. Recirculation method;
3. Flow method;
4. Synthetic method.

This provides a well-structured, classification according mainly to the feeding type and sampling method mainly. However, some authors prefer to elaborate this classification towards on how the compositions of the equilibrium phases are determined, analytically or not and whether the mixture to be investigated has been prepared (synthesized) with accurate composition known or not. This provides us with two classes:

1. Analytical methods;
2. Synthetic methods.



In each of these classes we can find many different methods divided into subclasses according to several experimental conditions (Figure 3.1). The variety of experimental methods reported is even more confusing, since various authors use different names for the same experimental method. Expressions like ‘static’ or ‘dynamic’ are used in connection with many different methods [2].

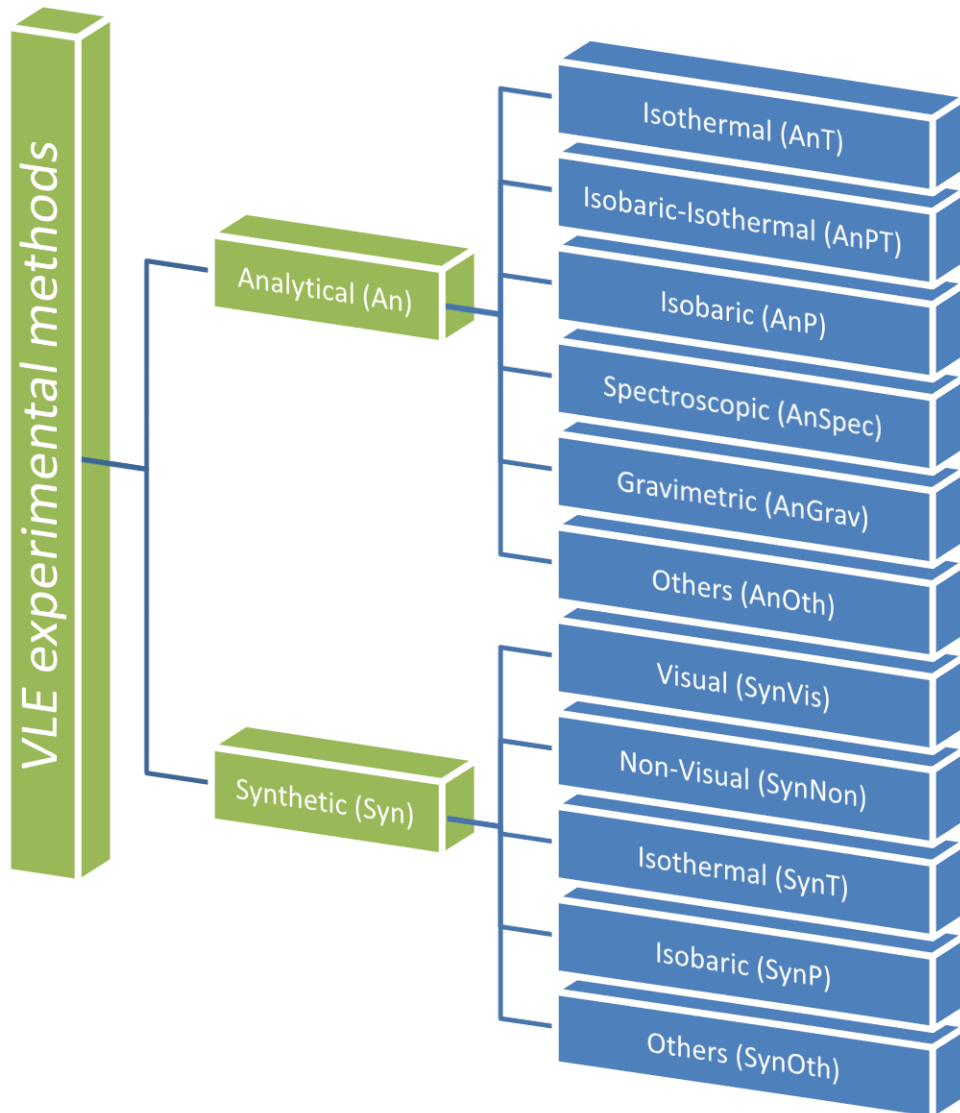
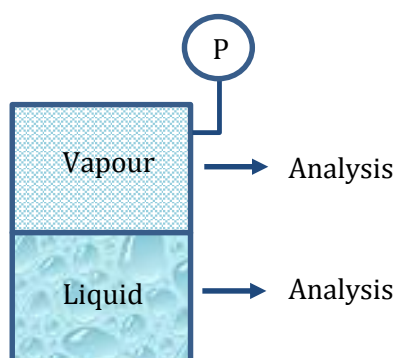


Figure 3.1 – Classification of experimental methods for VLE according to Dohrn *et al.* [3]

### 3.2. Static Method

The static method is illustrated in Figure 3.2. In this method the cell, with constant or variable volume, is filled with each substance and temperature and pressure are adjusted to allow the phase separation. Magnetic stirrers or rocking equipment are used to reach the equilibrium state. After that, samples are taken from both phases to be analyzed by appropriate techniques, such as Gas Chromatography (GC) and mass spectrometry.



**Figure 3.2 – Schematic diagram of a static apparatus for VLE measurements**

The static method for VLE experiments under high pressure, has inherently several problems such as sampling problems. By withdrawing a sample from the cell it can cause a change in the equilibrium state variables (pressure, temperature and composition). Also, due to the partial vaporization or condensation during sampling, the analyzed sample composition may not be the same as that in the equilibrium cell [1]. However, for more than 40 years, this type of apparatus became increasingly important with the development made by Gibbs and van Ness [4]. At that time many others followed [5-11] this new method in various ways. Kolbe and Gmehling [12] developed an apparatus using this method, capable of measurements of vapour-liquid equilibria up to 423K and 1MPa. This work was used by the scientific community for many years as a reference, and it was used to test our apparatus (see chapter 5 for Paper I).

Despite new advances for apparatus for vapour liquid equilibrium, the static method is still used today. Guo *et al.* [13] developed, for the analysis of vapour pressure and vapour + liquid equilibrium up to 400K and 3MPa, an apparatus based on the static

analytic method with an internal stirrer and view windows (Figure 3.3). With this apparatus, the authors report an improvement in the average absolute deviation of vapour phase mole fraction (AAD  $y$ ) in comparison with literature data. However, they obtained a higher average absolute relative deviation of pressure (AARD  $p$ ), due to the effect of sampling in the pressure.

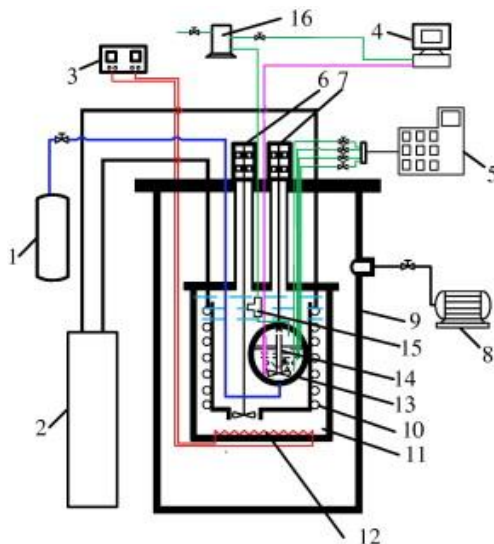


**Figure 3.3 – Schematic of the experimental apparatus of Guo *et al.* [13]. 1. Feed system; 2. Digital controller; 3. Digital controller; 4. Temperature and pressure indicator; 5. GC; 6 and 7. Motors; 8. Vacuum pump; 9. Vacuum vessel; 10. Cooling coil; 11. isothermal liquid bath; 12. Electric heater; 13. Equilibrium cell; 14. Stirrers; 15. Pressure transducer; 16. N<sub>2</sub>-filled system.**

### 3.3. Recirculation Method

A schematic diagram of recirculation apparatus is given in Figure 3.4. This method is based in the use of two recirculating pumps, one for the liquid and the other for the vapour phase. By recirculating the phase(s) the equilibrium state can be reached very fast and the disturbance of the equilibrium state inherent to sampling can be diminished using a special sampling device. When employing the recirculation method we must take care with the performance of the recirculating pumps and to the temperature of the bath in which all parts of the apparatus are placed.

These two reasons avoid the excessive pressure drop in the case of a good recirculating pump, and partial vaporization or condensation in recirculating lines.

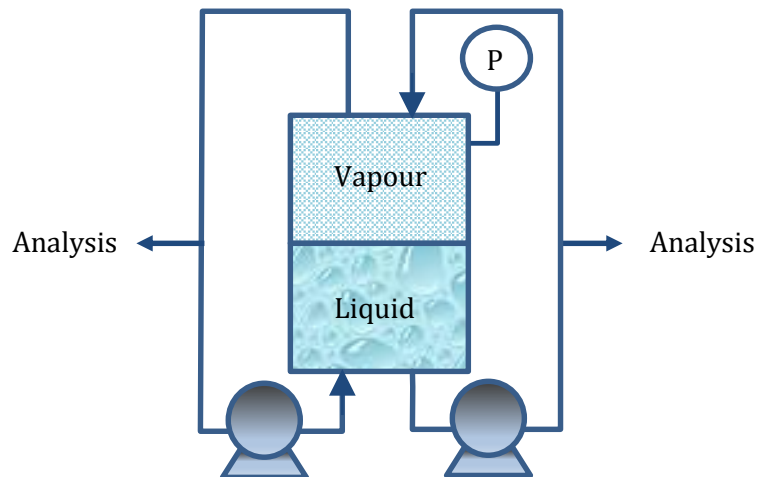


**Figure 3.4 Schematic diagram of a recirculation apparatus for VLE measurements**

In the work of Athès *et al.* [14], the authors report a problem with their deviation in temperature. In fact, the maximum temperature deviation at fixed liquid composition is of about 1.5 K. They attribute this deviation to some problems inherent to their recirculation method - Figure 3.5 - (partial condensation, pressure and temperature fluctuations) or to the uncertainty in the analysis of the ethanol composition.

These problems are very serious for VLE measurement in the region close to the critical point where a very small fluctuation in temperature and pressure can lead a big change in phase behavior [1].

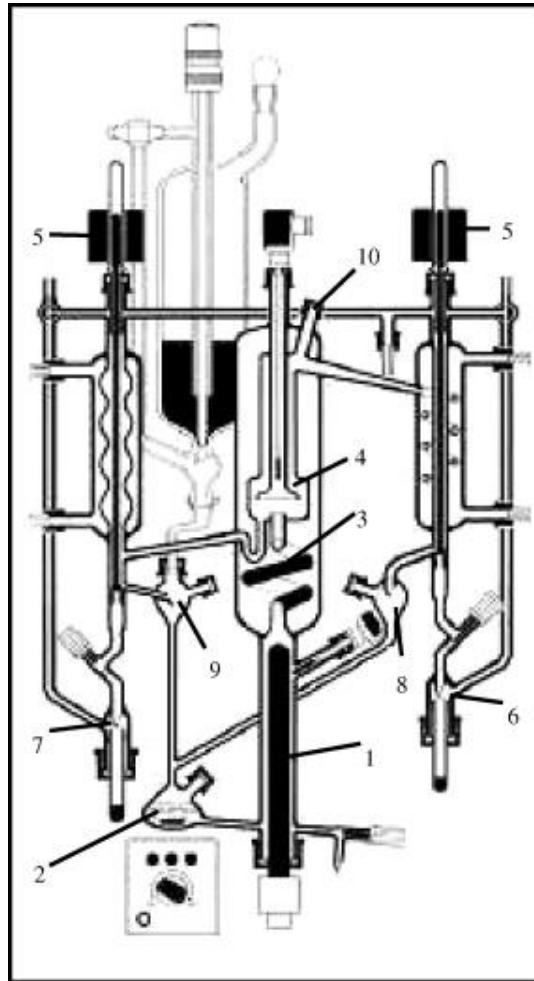


**Figure 3.5 - Flowchart of the vapour-liquid equilibrium apparatus Labodest® [14]** (1) electrical immersion heater; (2) mixing chamber; (3) contact path; (4) separation chamber; (5) solenoid valves; (6) vapour phase; (7) liquid phase; (8 and 9) circulation steams; (10) sampling port.

### 3.4. Synthetic Method

A schematic diagram of synthetic apparatus is given in Figure 3.4. This method is used to prepare a mixture of known composition (synthesize) and then to observe its behavior in a cell with visual observations. As shown in this figure, the synthetic method does not need sampling. After transferring the amounts of substances into the cell the temperature and pressure are adjusted until the contents of the cell form a homogeneous phase, whose mole fractions can be obtained from feed amount of each substance at the beginning. Then the pressure or temperature is varied until the incipient formation of a new phase.

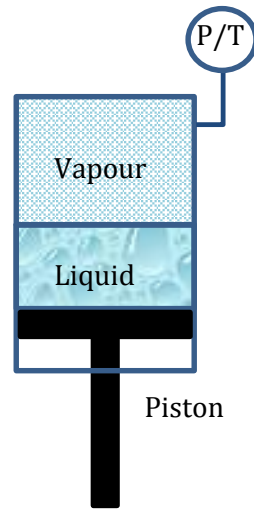


**Figure 3.6 – Schematic diagram of a synthetic apparatus for VLE measurements**

The known composition, the temperature and the pressure define a point of the phase envelope. The cell is usually of the variable volume type. The advantages of this method are that the difficulties regarding sampling are avoided, very simple apparatus is used, and that the phase envelope and PVT behavior of a mixture can be determined even near the critical conditions. However, the disadvantages are [1]:

- (1) Precise detection of incipient phase formation especially for dew point is difficult and it causes inaccuracies in temperature and pressure readings.
- (2) The composition of coexisting phases can only be determined indirectly in binary mixtures and in general cannot be obtained in multicomponent mixtures.

The synthetic method includes the so-called "dew- and bubble-point method" and also "total pressure measurement method". The former is just the same as that mentioned above and the latter is that where the amounts of substances transferred into the cell changed at constant temperature, until the formation of a new phase appears.

According to Fonseca *et al.* [2] in his review of the experimental methods and systems investigated in the period of 2005 to 2008, there is a tendency for

increasing the amount of papers using these types of methods. According to their review they are more used by the scientific community than the Analytical methods.

These methods can be used where the analytical methods fail, i.e., when phase separation is difficult, due to similar densities of the coexisting phases, e.g. near or even at critical points. Often the experimental procedure is easy and quick, and because no sampling is necessary, the equipment is rather inexpensive. On the other hand, it can be designed for extreme experimental conditions, as higher temperatures and pressures rise the costs of equipment.

A disadvantage of this method is that they yield less information than the analytical ones, being mainly used for binary or pseudo-binary mixtures [2].

A new experimental set-up for the measurement of phase equilibria at temperatures ranging from 243 K to 353 K and pressures up to 20 MPa was developed by Fonseca and von Solms [15], making use of the synthetic isothermal method. A schematic representation of the apparatus is presented in Figure 3.7.

The quality of this equipment was confirmed by the authors through several tests, including measurements along the three phase co-existence line for the system ethane + methanol, the study of the solubility of methane in water, and of carbon dioxide in water. They found that the largest influence on the accuracy of the solubility results is related to the ratio between the volumes of the two phases in equilibrium. Experiments with small volume of the vapour phase are less susceptible to the influence of other sources of errors, resulting in a higher precision of the final results.

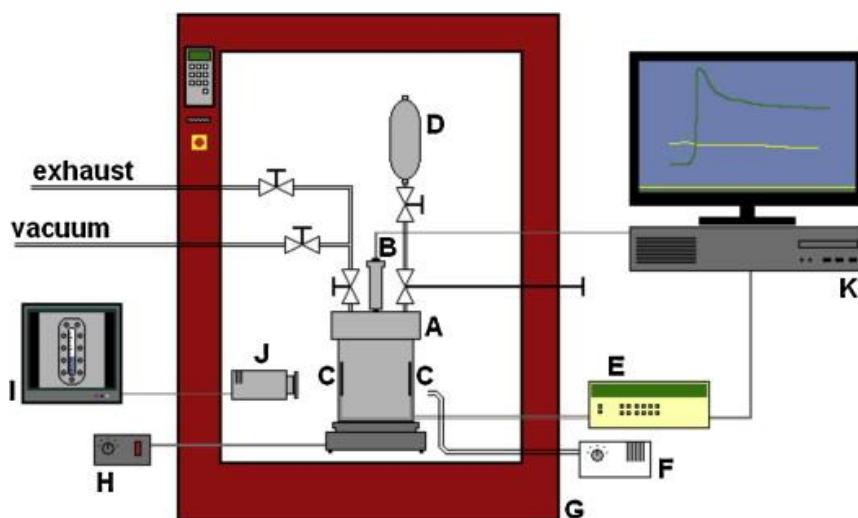


Figure 3.7 - Schematic representation of the new experimental set-up for the measurement of multi-phase equilibria by a synthetic method. (A) High-pressure view cell. (B) Pressure sensor. (C) Platinum resistance thermometers. (D) High-pressure gas cylinder. (E) Data logger. (F) Cold light source with optical fibre (G) Temperature chamber. (H) Stirring with remote control. (I) Video monitor. (J) Video camera. (K) Computer for data acquisition [16].

### 3.5. Flow Method

A schematic diagram of the flow method is illustrated in Figure 3.8. This is an open cell, in which flows two or more components are flowing continuously in the cell, until steady-state is reached. This technique offers several advantages, mainly a short residence time in the cell (avoiding thermal degradation) and the possibility of obtaining large amount of samples of both phases. However, the flow method is a dynamic system and it has some problems [1]:

- (1) The precise control of both feed rate and liquid level in a cell must be done in order to keep the masses of components fixed;
- (2) A suitable sampling technique should be developed to collect complete sample, especially for multicomponent mixtures;



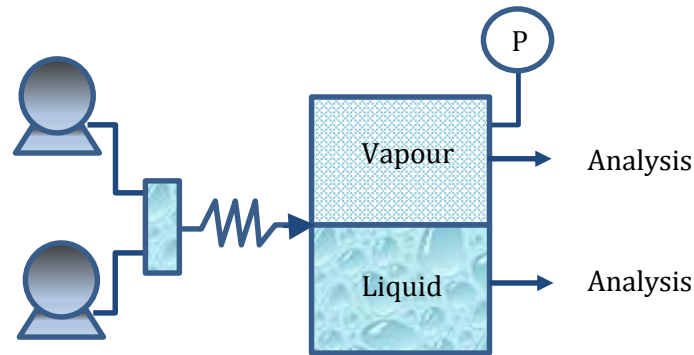


Figure 3.8 Schematic diagram of a flow apparatus for VLE measurements

An application of this method developed by Niesen *et al.* [15] is shown in Figure 3.9.

The precise control of both feed rate and liquid level in a cell can be achieved once known how both the feeding pump and the exiting valves work. Despite of this method being a flow method it can easily be upgraded to a recirculating flow method whenever the quantity of the original sample is in question. To avoid the excessive pressure drop a back pressure regulator can be installed diminishing the effects in the equilibrium.

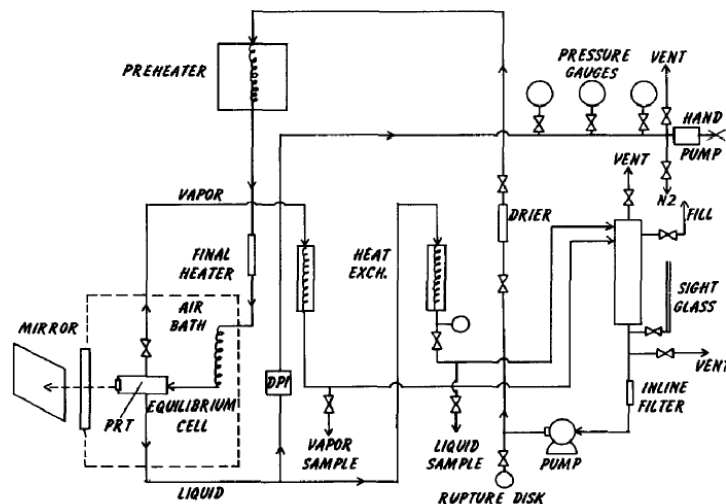


Figure 3.9 -Vapour liquid equilibrium apparatus of Niesen *et al.* [15] based on a flow method

For this work, and according to the classification of Nagahama this Flow Method was chosen to design our VLE apparatus. The main reason of this option is the minimization of possible thermal degradation, since the residence time of the mixture in the VLE cell is highly reduced.

### **3.6. Bibliography**

- [1]. K. Nagahama, *Fluid Phase Equilibria* 116 (1996) 361-372
- [2]. R. Dohrn, S. Peper, J.M.S. Fonseca, *Fluid Phase Equilibria* 288 (2010) 1-54
- [3]. R. Dohrn and G. Brunner, *Fluid Phase Equilibria* 106 (1995) 213-282
- [4]. R.E. Gibbs and H.C. Van Ness, *Ind. Eng. Chem. Fundam.* 11 (1972) 410-413
- [5]. M. Ronc and G.R. Ratcliff, *Can. J. Chem. Eng.* 54 (1976) 326-332
- [6]. R.P. Tomlins and R.N. Marsh, *J. Chem. Thermodyn.* 8 (1976) 1195-1197
- [7]. K. Aim, *Fluid Phase Equilibria*, 2 (1978) 119-142
- [8]. P.J. Maher and B.D. Smith, *J. Chem. Eng. Data*, 24 (1979) 16-22
- [9]. D. Legret, D. Richon and H. Renon, *Ind. Eng. Chem. Fundam.* 19 (1980) 122-126
- [10]. A. Tamir, A. Apelblat and M. Wagner, *Fluid Phase Equilibria*, 6 (1981) 237-259
- [11]. R.A. Mentzer, R.A. Greenkorn, and K.C. Chao, *J. Chem. Thermodyn.* 14 (1982) 817-830
- [12]. B. Kolbe and J. Gmehling, *J. Fluid Phase Equilibria*, 23 (1985) 213-226
- [13]. H. Guo, M. Gong, X. Dong and J. Wu, *J. Chem. Thermodynamics* 76 (2014) 116-123
- [14]. V. Athès, P. Paricaud, M. Ellaite, I. Souchon and W. Fürst, *Fluid Phase Equilibria*, 265 (2008) 139-154
- [15]. V. Niesen, A. Palavra, A.J. Kidnay and V.F. Yesavage, *Fluid Phase Equilibria*, 31 (1986) 283
- [16]. J.M.S. Fonseca and N. von Solms, *J. of Supercritical Fluids*, 86 (2014) 49-56

## **Chapter 4 – VLE apparatus and Experimental Procedure**

In this work a vapour-liquid equilibrium (VLE) continuous flow apparatus was used. The purpose of using continuous flow apparatus, as said before, is to minimize thermal decomposition in the phases under study. Originally constructed by Rosa *et al.* [1], and upgraded for this study, this apparatus was designed to collect vapour-liquid equilibrium data at temperatures up to 453.15K and pressures up to 1.7MPa. A second apparatus was built to extend the ranges of temperatures up to 573.15K and pressures up to 20MPa. Both instruments are described in this chapter.

### **4.1. Vapour-Liquid Equilibria Apparatus #1**

The first VLE apparatus used in this study is presented schematically in Figure 4.1 and shown in Figure 4.2. It is the same apparatus as that described and tested by Rosa *et al.* [1], subjected to modifications in the pressure transducers and in the oven stability in order to allow more accurate measurements. There are three main sections in this apparatus: sample feeding section, equilibrium section and sampling section.

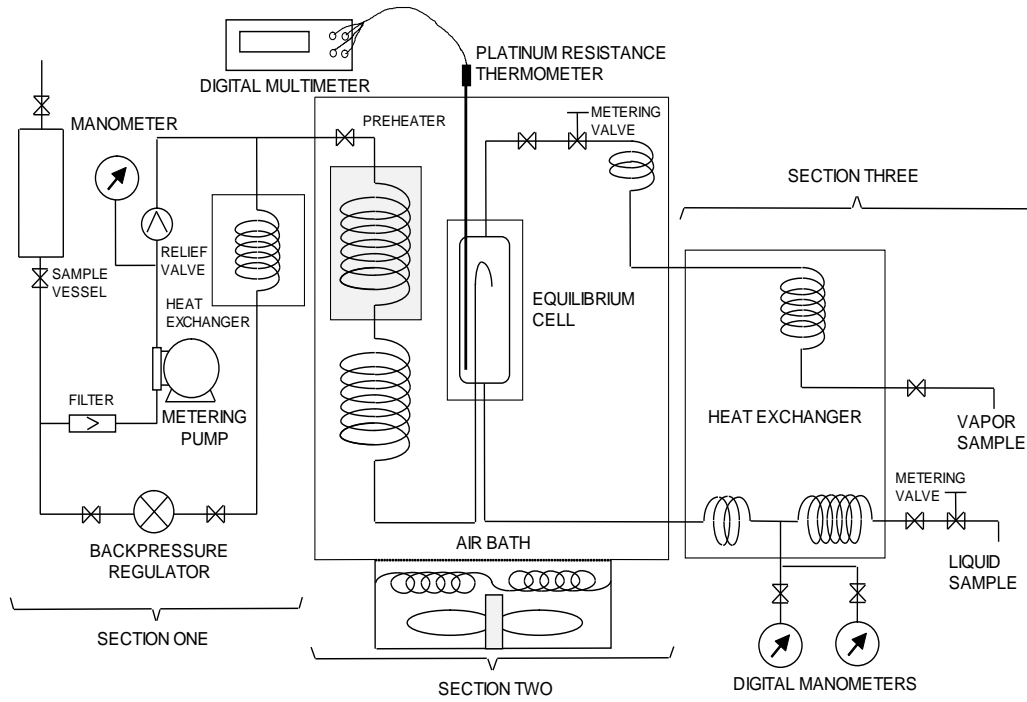


Figure 4.1 - Schematic of the VLE apparatus #1[1]

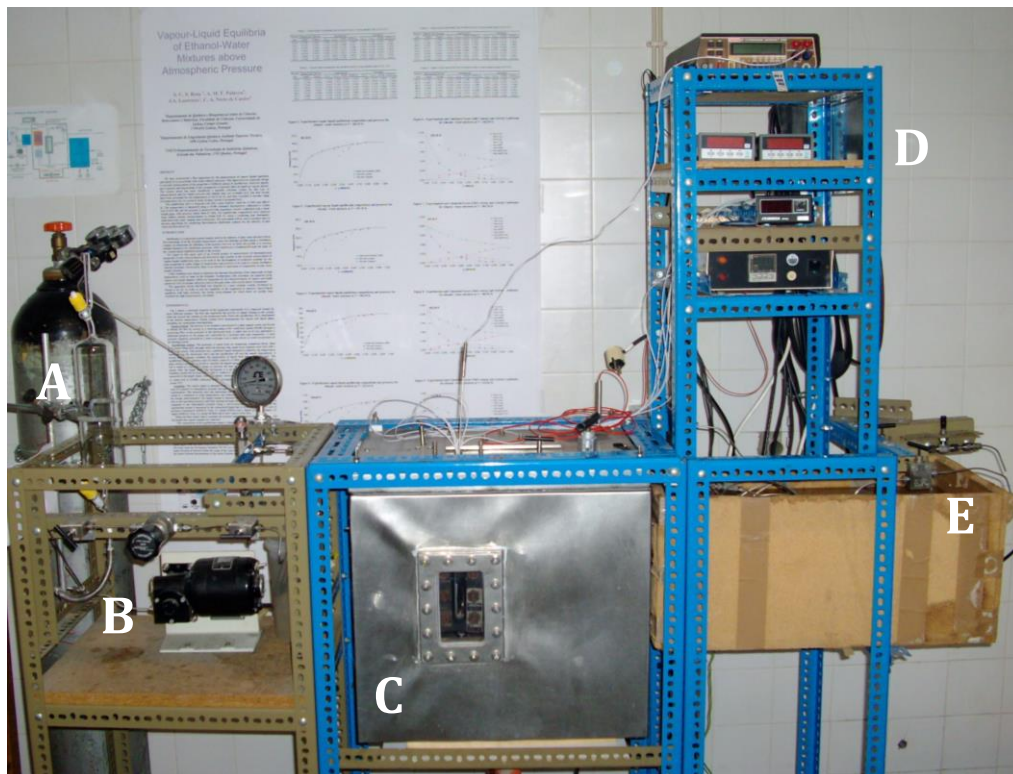
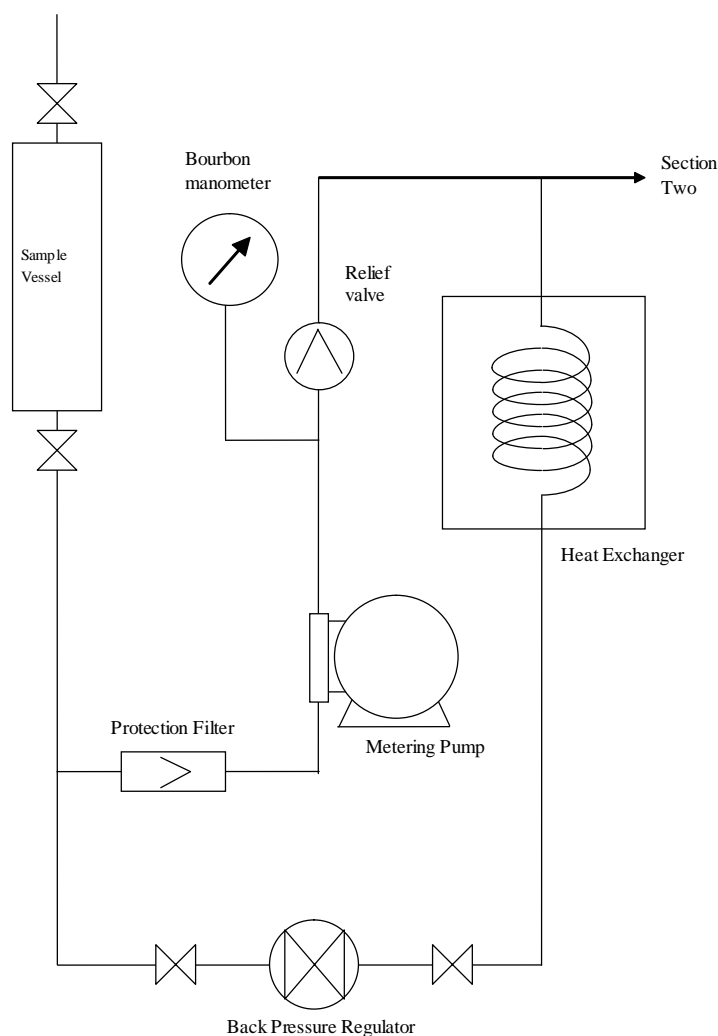


Figure 4.2 - Overall view of VLE apparatus #1. A - feeding vessel; B - circulating pump; C - oven with window; D - Measurement and control zone; E - Sampling zone.

#### 4.1.1. Sample feeding section

Figure 4.3 shows a schematic diagram of this section. The mixture to be studied is introduced in a glass sample vessel, and forced to initiate the flow by suction by a metering pump (LDC Analytical, model 396-89) through a protecting filter, to the preheater in the thermostat bath in section two. A relief valve in its way guaranties a minimum pressure at the pump exit, controlled by a Bourdon tube type manometer. A back pressure regulator, preceded by a heat exchanger, acts a safety device to avoid overpressure in the flowing system.



**Figure 4.3 – Schematic of the sample feeding section of the VLE apparatus #1 [1]**

#### 4.1.2. *Equilibrium section*

This section (Figure 4.4) consists on an isothermal air bath, containing the preheater and the equilibrium cell which is maintained at the desired temperature. The preheater is made from an aluminum cylindrical block, filled with copper filing dust, through which the flowing tube, made from stainless steel 316S (OD = 0.3175 cm) passes. This preheater has a sufficient length designed to minimize the temperature shock between the thermostat entry and the equilibrium cell and the sample degradation. A second heat exchanger stabilizes the temperature of liquid fluid before the cell entry. The equilibrium cell (Figure 4.5) is a stainless steel 316 block, rated for 13MPa and 588.15 K, equipped with a glass window (Jerguson 11-R-20) to visualize the liquid-vapour interface. The input line to the cell is made in an inverted U shape, to increase the heat and mass transfer between the two phases after the liquid flash. The thermostat is an air-bath controlled by a PID controller (OmRon, model E5CN) from 303.15K to 523.15K, within  $\pm 0.5\%$  of indicated value given by supplier. The temperature of the equilibrium is measured inside the high pressure cell, with the thermometer in the liquid phase, with a platinum resistance thermometer (OMEGA Tech. Co), and a 5½ digit multimeter (Keithley, model 197) calibrated together by Electrónica Industrial de Alverca (EIA) (see Appendix 1 for calibration certificate) with an expanded uncertainty 0.049K (k=2) for the Temperature working range.

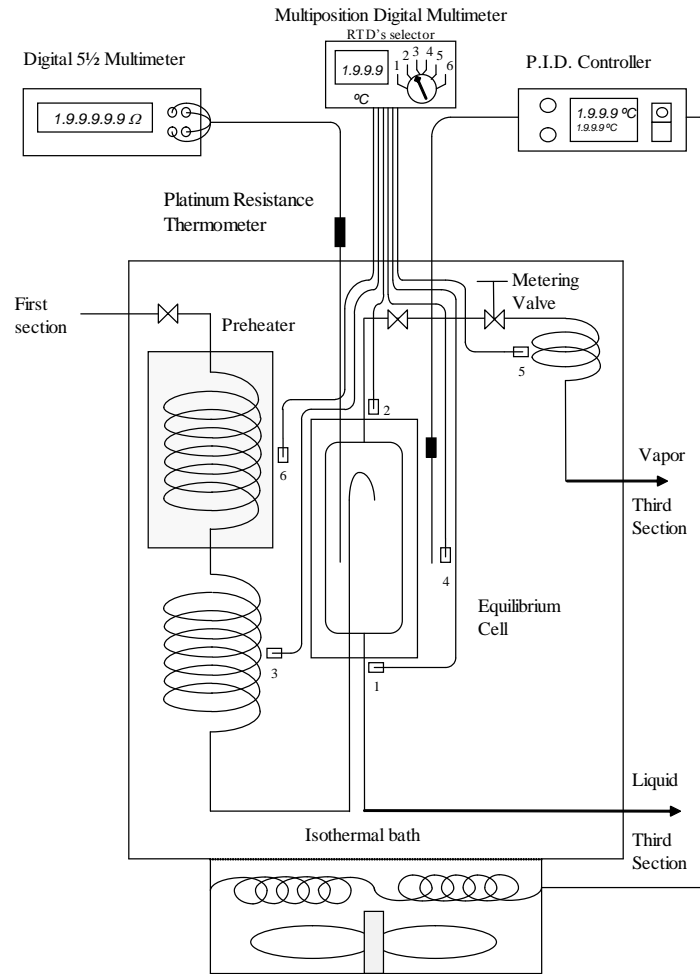


Figure 4.4 – Schematic of the equilibrium section of the VLE apparatus #1 [1]



Figure 4.5– View of the high pressure cell of VLE apparatus #1

#### 4.1.3. Sampling section

This section of the apparatus is schematically represented in Figure 4.6. The vapour phase is sampled from the top of the cell, using a micro-metering valve to expand it to atmospheric pressure through a coil inside the thermostat to prevent pre-condensation. This metering valve also determines the vapour flow rate. The vapour is then cooled in a condenser (heat exchanger) to room temperature, and collected in a small glass flask, prepared for the density determination. The liquid sample is obtained from the bottom of the equilibrium cell, at the operating pressure, and after passing through the condenser where it cools down, is expanded to the atmospheric pressure using a micro-metering valve.

When the steady-state is reached the pressure of the equilibrium system is measured in the compressed liquid line with a pair of pressure transducers (GE Druck, model UNIK5000) with 0-0.4 and 0-1.7MPa calibrated by the manufacture with uncertainties<sup>2</sup> of  $\pm 0.02$  and  $\pm 0.085$  MPa respectively, and a digital pressure readout, 4½ digits (GE Druck model DPI282). The composition of the equilibrium sample is determined by densimetry, using a (Anton Paar DSA 5000 M) densimeter<sup>3</sup>.

The values of the density of the binary mixtures of ethanol–water were obtained from published data and fitted to a polynomials in the molar fraction of ethanol within the range of the experimental measurements (see Appendix 2). The uncertainty of the molar fraction determination, taking into account the uncertainty in the density measurements was found to be  $u_x = 0.0001$ . The same procedure was adopted for the other two binary mixtures.

---

<sup>2</sup> Uncertainty of 0,05% full-scale given by the manufacture

<sup>3</sup> Calibrated with water (Millipore) and tetrachloroethylene (H&D Fitzgerald - certified values) with an expanded uncertainty of 0.01 kg m<sup>-3</sup> (k =2) [2]



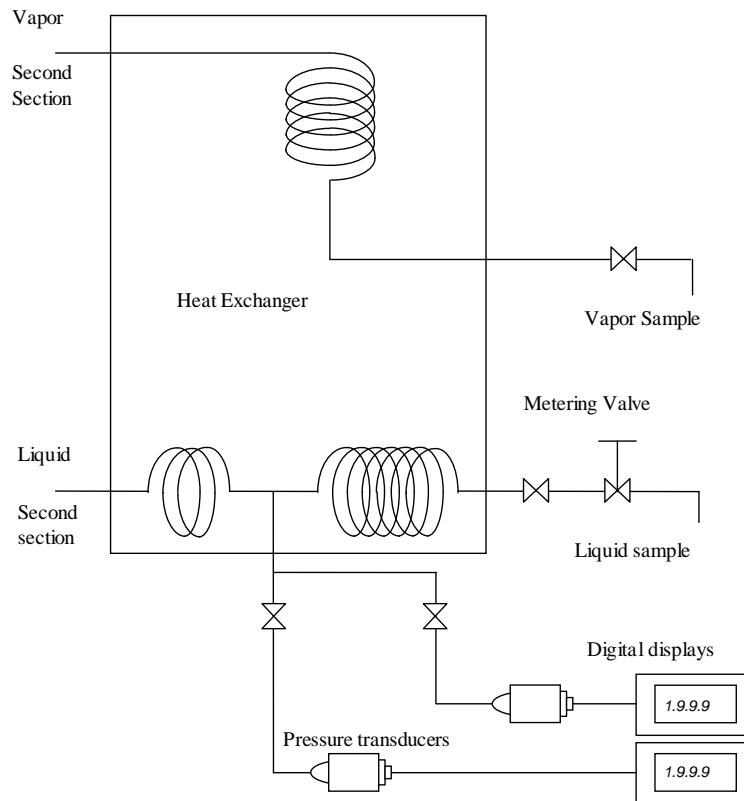


Figure 4.6 – Schematic of the sampling section of the VLE apparatus #1 [1]

#### 4.2. Evaluation and Testing of the VLE Apparatus #1 performance

In this section all the upgrades, evaluations and tests conducted to the vapour-liquid equilibrium apparatus #1 in the first year of this thesis are described. These tests were carried out in order to better understanding the limitations of the equipment and to try to minimize variations in equilibrium, due to the operational procedure. For this, the tests carried out to the circulating pump, to the air bath and to the collecting valves are presented. To test the performance of the apparatus the water-ethanol system was chosen, since there are accurate data for it obtained by Niesen *et al.* [3]. The study was carried out at 423.7K and the agreement between both data, as shown in detailed in Chapter 5, in Paper I suggested the good performance of the apparatus.

#### 4.2.1. LDC Analytical Pump, model 396-74

As described in chapter 3, the flow method has the advantage of short residence time in the cell avoiding thermal degradation and the possibility of obtaining large amount of samples of both phases. However, the accurate control of both feed rate and liquid level in a cell must be done in order to keep the masses of components fixed. Whenever the flow rate changes, there is a direct perturbation in the system resulting in variations in both temperature and pressure as well in the mass of each component. So, in order to minimize these perturbations, a test was performed to the circulating pump to better understand the effect of changing the flow during the experimental procedure.

The model used in this equipment provides us a variation of feeding between 0 and 100% flow. For these extremes we have a corresponding flow velocity of 0.63 and 6.38 ml.min<sup>-1</sup> given by supplier. The equation that gives us the flow rate is given by:

$$v(\text{ml. min}^{-1}) = 0.0575 \times \text{flow}(\%) + 0.6333 \quad \text{equation 4.1}$$

In tests carried out with pure ethanol the optimal feeding flow rate was found to be between 15 to 30%. For minor flow rates the cell would take too much time to fill and almost all the liquid entering the cell would vaporize. For higher flows the perturbation in the pressure was higher giving higher vapour pressure values. It was found that in this case it was very difficult to fix the temperature. But for the control of the level in the equilibrium cell the feeding is not the only variable affecting this, the sampling is also a big problem. The equilibrium between the entering and exiting of a sample must be in perfect harmony. For this in the next section we talk about the optimization of the sampling valves.

#### 4.2.2. Micro-metering Valves

As mentioned in the description of the ELV apparatus, there are two micro-metering valves for collection of the gas and liquid phase samples. In order to try to establish a correspondence between the opening in the valve and the amount of ejected sample (ml) per unit time (minute), to acquire an equilibrium between the input and

output of the samples, tests were performed making it possible to express this relationship in equation 4.2 for liquid and equation 4.3 for vapour phases

$$v(\text{ml} \cdot \text{min}^{-1}) = 8.1657 \times \text{opening} - 2.5674 \quad \text{equation 4.2}$$

$$v(\text{ml} \cdot \text{min}^{-1}) = 3.7921 \times \text{opening} - 0.3298 \quad \text{equation 4.3}$$

These tests were conducted with a fixed input of 30% in the feeding pump, considerer the optimal feeding flow. Each time the opening of a valve was changed, an alteration in the equilibrium would occur; for minor openings there was an increment in the vapour pressures. For an input of 30% we found that for achieving equilibrium in the cell level we had to have equilibrium between the amounts of both exiting phases for low temperature values. For higher temperatures and for the same feeding flow we had more vapour in the system, so the opening of the vapour valve was consequently higher. These relations were based in experience of developing an optimal relation between feeding and sampling.

#### 4.2.3. *Air Bath*

As already mentioned, the VLE apparatus was constructed with an air bath to control the temperature of the cell. The reason for choosing this over a liquid heat transfer fluid (i.e. oil), which is more stable and not subject to the big convection currents, is based on the fact that for higher temperatures and with time the oil degrades sometimes with toxic products, making it difficult to observe the liquid-vapour interface in the equilibrium cell. Another reason, no less important, is because of the industrialization process, that for a large scale industry, oils become expensive as industrial heating requires high volumes. Moreover, some oils used at high temperatures are usually toxic.

The PID controller present in the bath with an uncertainty within  $\pm 0.5\%$  of indicated value given by supplier, for temperatures of 423.2K we had uncertainties of 2.1K. Despite this the temperature of the equilibrium was measured in the liquid phase with a platinum resistance thermometer inside the equilibrium cell, with a much better uncertainty.

In order to assess the stability of the air bath experiments were performed at room temperature and at 423.15K. In this evaluation temperature readings were obtained from the six RTD displayed in specific places as shown in Figure 4.4. Each reading was the average of ten temperature readings (spaced by 1 minute) after two hours of stabilization. For the room temperature tests, the control temperature was the laboratory ambient temperature. For higher temperatures the control temperature was the PID controller temperature. For the standard of each RTD the temperatures of the six of them were registered with the air bath opened (for values see Appendix 3).

By introducing steel mesh, we observe a stabilizing the bath at higher temperatures, since it decreases the convection. However, despite of this it is extremely difficult to avoid the heterogeneous filling of the air bath. As it can be seen in Figure 4.7 the introduction of the steel mesh at room temperature stabilizes the temperature readings between the RTD's but increases the difference between the room temperature and the RTD's readings. In Figure 4.8 we can also see that for 423.15K the temperature between the Standard and RTD's are higher than  $\pm 5$  K (for values see Appendix 2). This makes the filling more problematic than helpful.

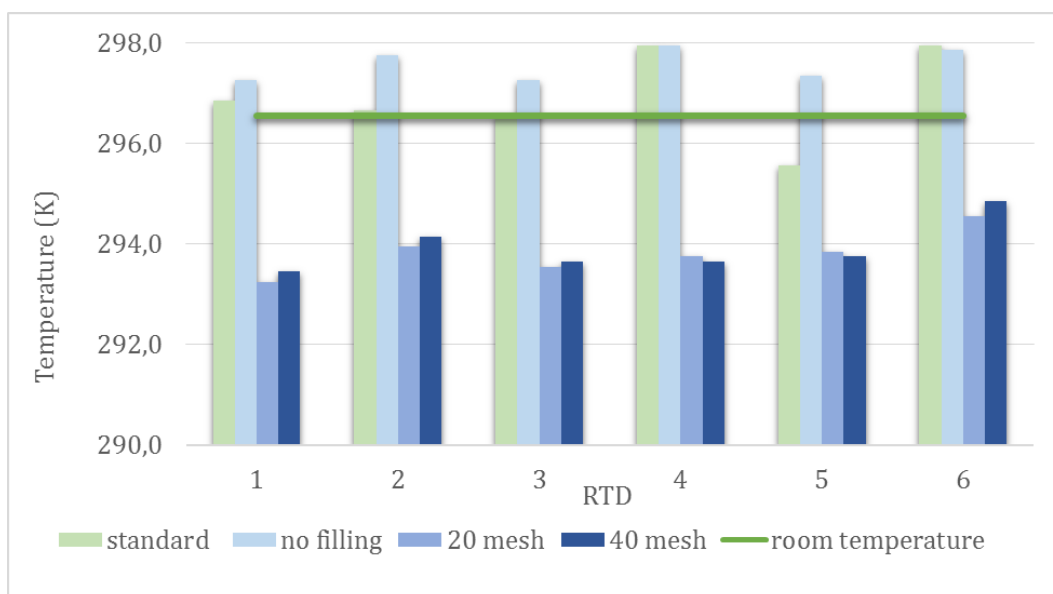


**Figure 4.7 – Stability of the air bath at 296.55K without any filling or with steel mesh filling in comparison with the temperature measured with the open bath (standard).**

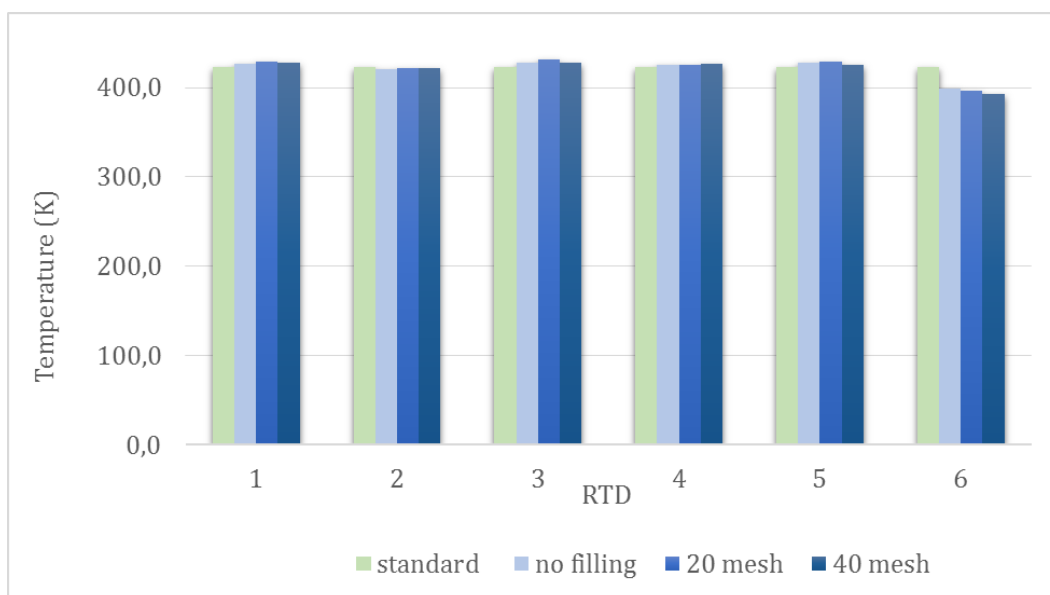


**Figure 4.8 – Stability of the air bath at 423.15K without any filling or with steel mesh in comparison with the PID controller temperature (standard).**

### 4.3. Vapour-Liquid Equilibria Apparatus #2

A second VLE flow apparatus was built to extend the VLE measurements up to 20MPa at a maximum temperature of 573.15K (Figure 4.9). It represents a development of the original one (apparatus #1), allowing more accurate measurements. Although similar in the design, it presents some differences in the mentioned three sections.

In the sample feeding section we have a glass sample vessel, where the mixture is present and forced to initiate the flow by suction by a similar metering pump (LDC Analytical, model 396-89) through a protecting filter, to the oven in section two. In this section we don't have a relief valve, but a bourdon tube type manometer gives us the pressure value at the pump exit. A back pressure regulator acts a safety device to avoid overpressure in the flowing system.

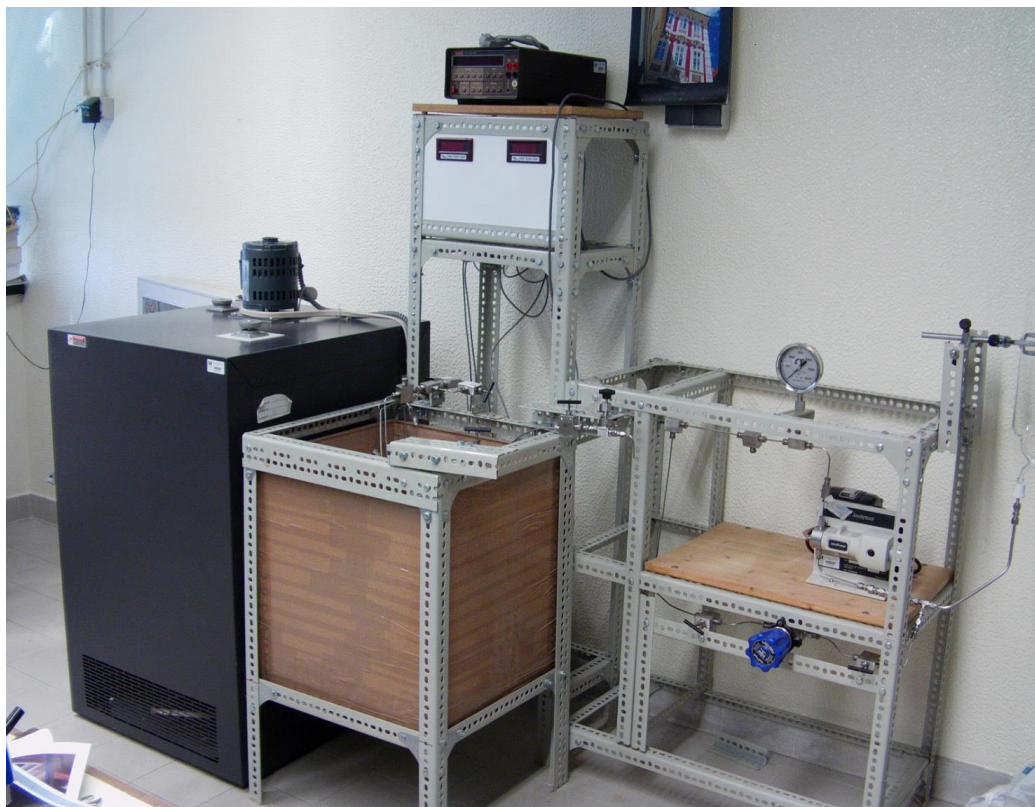


**Figure 4.9- VLE apparatus #2**

In this apparatus an oven (Hotpack, model 213024) capable of reaching 623,15K containing the equilibrium cell will represent the equilibrium section. Once inside this oven, the sample will pass by a 24m spiral of tubing (1/8" O.D.) serving as a preheater, and then enter the high pressure cell.

In the original high pressure cell the seal in the glass window is done through a Teflon<sup>®</sup> gasket. Since the Teflon<sup>®</sup> cannot be used above 450 K, a new high pressure cell was designed, which is shown in Figure 4.10.

The cell is constructed from a cylindrical block of 316SS. The view port is a 4.445 cm diameter by 0.635 cm thick sapphire window (Figure 4.10a). A 0.101 cm diameter, 24 K gold o-ring will seal the sapphire window, making a tight seal due to the pressure apply to this o-ring. The opposite end of the cell will have a dummy window which is made of 316SS, and that will be seal with another 24 K gold o-ring. Brass backup shims will be used to hold the o-rings in place and to eventually distribute the sealing force around the outer edge of the windows. Belleville washers are used

to counteract thermal expansion effects. Figure 4.10b shows a schematic of an upper view cut of the cell and Figure 4.11 the cell under construction inside the oven.

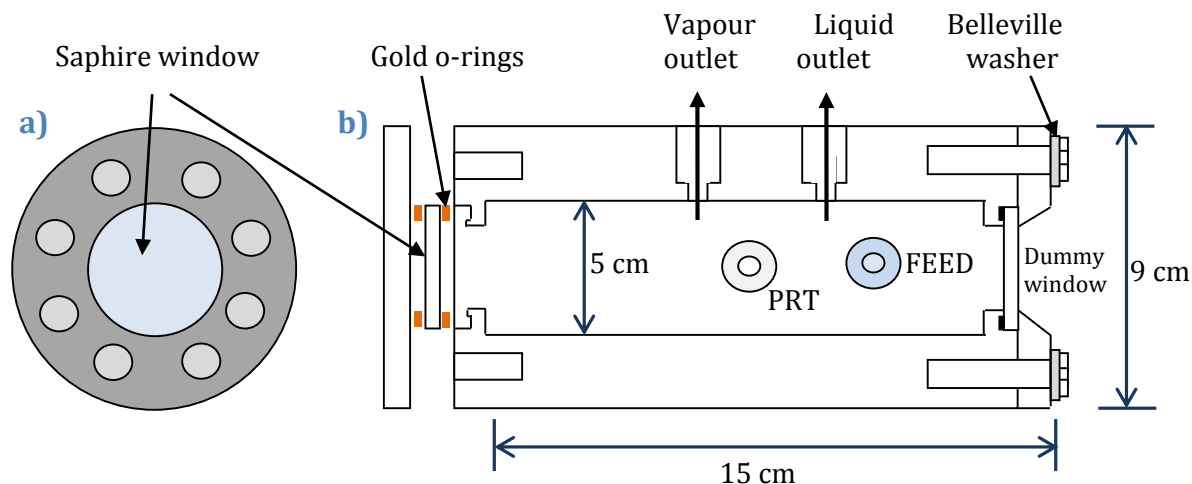


**Figure 4.10 - a) Frontal view of the high pressure equilibrium cell of the VLE apparatus #2, and b) upper cut view of the cell.**

To carry out temperature measurements up to 573.15 K, a commercial oven (Hotpack, model 213024) was used. Due to a better temperature control inside the oven ( $\pm 0.1$  K given by supplier), more accurate temperature measurements can be achieved.

The temperature of the equilibrium will be measured inside the high pressure cell, in the liquid phase with a platinum resistance thermometer (Wika model CTH7000) calibrated by manufacture to within  $\pm 0.05$  K (given by calibration – see appendix 1 for calibration certificate), and the resistance will be measured with a 5½ digit multimeter (Keithley, model 196), better than before.

Once the equilibrium is reached, the vapour and the liquid samples are collected in the sampling section, and the pressure and temperature values are measured. The pressure with the pressure transducers (Setra Systems, Inc., model 206) with 0-6,89 and 0-20,7MPa (no calibration available yet) and digital pressure readouts, 4½ digits (Setra Systems, Inc., model 300D).

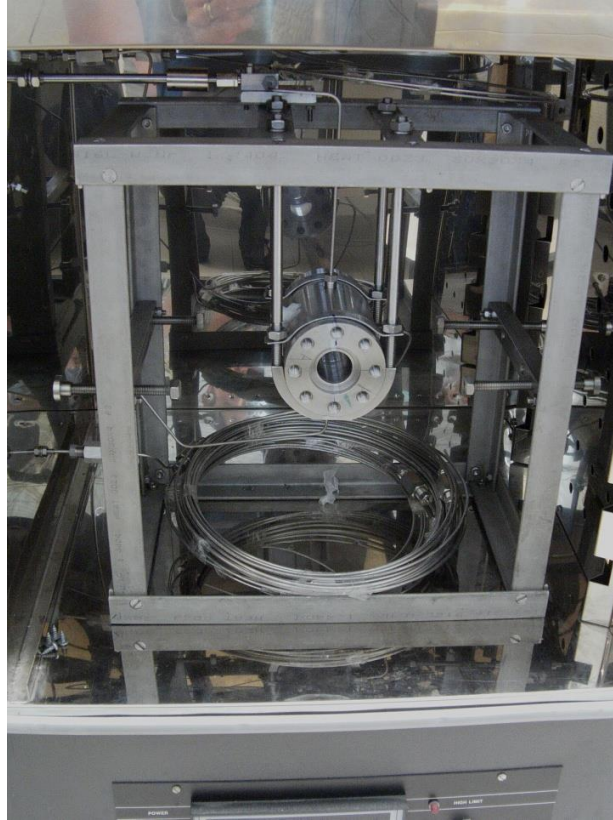


**Figure 4.11 – High pressure equilibrium cell of the VLE Apparatus #2**

#### **4.4. General operating instructions of the VLE apparatus and experimental procedure**

It is important to understand that for VLE measurements is more difficult to operate a flow system than a static one. The equilibrium state required for the measurements must be achieved and maintained in a flow system in contrast to a more stable batch system. For example, the temperature of a bath is much easier to control than the temperature of a fluid flowing through a tube of 1/8" O.D. at 100ml/min. For a binary system there are two degrees of freedom. Additionally, there is the obvious requirement that when the steady-state is reached, relative proportion of the two phases should be maintained. For this equipment, the temperature and vapour/liquid meniscus are controlled requiring the pressure to be fixed and by setting the flow rates of the two phases.



#### *4.4.1. Starting*

The first thing to do when starting from zero operating the VLE apparatus is to turn on the entire electrical system, and the multimeter and let it stabilize for a while. Then all valves should be checked, all valves should be opened with exception of the vapour and liquid exit valves (the access valves to the transducers should be opened carefully). Then the PID controller, or the oven controller (in case of VLE#2) should be turned on and the temperature should be insert. After these initial tasks, the system is now ready for stabilize the temperature. After approximately 1 hour of temperature stability, the pump is turned on in the minimum flow. In case of VLE#1 it can be established the exit pressure of the fluid with the relief valve. In this stage the cell will start to fill. The back pressure (that can be closed for a filling more rapid of the cell) should be regulated for the maximum exit pressure of the pump, acting as a safety device to avoid overpressure in the flowing system. The liquid level should be maintained controlling the vapour exit valve.

#### *4.4.2. Equilibrium*

This is the more difficult stage to operate. The liquid level should be maintained by controlling the vapour and liquid exit valves, the pump flow and the back pressure regulator, in order to have the same quantity of sample at entry and exit of the apparatus (steady-state mass flow). In practice, this is difficult because at minimum de-regulation in one of these possible controlling parameters, the equilibrium is perturbed and the level of liquid varies.

#### *4.4.3. Sampling*

After about 15 minutes (maximum time calculated with the minimum flow rate for the fluid to reach the end of the system) with the system is equilibrium, samples of the vapour and liquid phase can be collected. . Samples are collected in glass flasks in ice baths for minimize the sample evaporation. As mentioned in section 4.1.3. the composition of the equilibrium sample was determined by densimetry, using a densimeter. The values of the density of the binary mixtures were obtained from published data (see references in Papers I, II and III) and fitted to polynomials in the

molar fraction of ethanol within the range of the experimental measurements (for values see Appendix 2).

#### *4.4.4. Turning off*

When finished the fluid flow is turned to zero, as well as the pump. Then the PID controller or the oven is turned off, and all valves closed after a while with exception of the transducers valves. The temperature and pressure of the system is controlled to guaranty that it decreases safely. If necessary the exit valves are opened to decrease the pressure and consequently the temperature more rapidly in the system, but these valves should be closed in the end.

## **4.5. Bibliography**

- [1]. S.C.S. Rosa, C.A. Nieto de Castro, A.M.F. Palavra, Proceedings of 4th Asian Thermophysical Properties Conference (1995) 467–470
- [2]. I.M.S. Lampreia and C.A. Nieto de Castro, Journal Chem. Thermodyn. 43 (2011) 537-545
- [3]. V. Niesen, A. Palavra, A.J. Kidnay and V.F. Yesavage, Fluid Phase Equilibria, 31 (1986) 283

## Chapter 5 – Results and Discussion

In this chapter details about the experimental results and discussion are presented in article format. Articles are referred as “Paper I”, etc.

### 5.1. List of Papers

#### Paper I.

A.F. Cristino, S. Rosa, P. Morgado, A. Galindo, E. J. M. Filipe, A. M. F. Palavra and C. A. Nieto de Castro, *High-temperature vapour-liquid equilibrium for the water-alcohol systems and modeling with SAFT-VR: 1. Water-ethanol*, Fluid Phase Equilib. 341 (2013) 48-53  
doi:10.1016/j.fluid.2012.12.014

#### Paper II.

A.F. Cristino, S. Rosa, P. Morgado, A. Galindo, E. J. M. Filipe, A. M. F. Palavra and C. A. Nieto de Castro, *High-temperature vapour-liquid equilibrium for the water-alcohol systems and modeling with SAFT-VR: 1. Water-1-propanol*, J. Chem. Thermodyn. 60 (2013) 15-18  
doi:10.1016/j.jct.2012.12.019

#### Paper III.

A.F. Cristino, P. Morgado, A. Galindo, E. J. M. Filipe, A. M. F. Palavra and C. A. Nieto de Castro, *High-temperature vapour-liquid equilibrium for ethanol-1-propanol mixtures and modeling with SAFT-VR*, Submitted to Fluid Phase Equilibria

## 5.2. Summary of Papers

A flow apparatus originally built in the Faculty of Sciences from Lisbon University was upgraded and tested to carry out vapour-liquid equilibrium at high temperatures for water-alcohol binary mixtures in the temperature range of 363–443 K and pressures up to 1.7 MPa. In **Paper I** experimental VLE data for the water-ethanol system is presented for temperatures between 363.3 and 423.7 K, and pressures up to 1 MPa. The results obtained were compared with available literature data to test the accuracy of the equipment and also with the predictions from SAFT-VR EOS. The performance of this VLE apparatus was found to be commensurate with the design parameters and the required accuracy.

**Paper II** is dedicated to the vapour-liquid equilibrium of the water-1-propanol binary mixture for temperatures between 403.2 and 423.2K, and pressures up to 0.72MPa. Vapour pressures for the pure 1-propanol were also obtained in the temperature range from 383.2 to 423.2K and compared with literature. Once again the agreement between experimental results and data from the literature was excellent being the deviation in the vapour pressure of pure propanol well within the mutual uncertainty of the vapour pressure, except at the highest temperature, where our value is 0.01 MPa higher. In all the experiments this temperature was found to be the more unstable due to the limits of pressure and temperature that the apparatus is under.

The SAFT-VR was found to be a good tool to predict the behavior of this binary mixture. However, the values of the binary interaction parameters were only slightly adjusted from those obtained for the (water + ethanol) system in order to obtain better predictions.

In order to complete the cycle of binary mixtures using water, ethanol and 1-propanol, in **Paper III**, experimental vapour liquid equilibrium data for the ethanol-1-propanol binary mixture was obtained using the same flow apparatus. The SAFT-

VT has proven as in Paper I that overestimates the vapour pressure for pure ethanol. This fact was investigated in this paper, using the Wagner equation for pure ethanol as well as for pure 1-propanol, since the accurate representation of vapour pressure data over a wide temperature range requires an equation of greater complexity. The good agreement of previous experimental determinations and results from the literature with this equation supported the idea that it is one of the most effective in modelling the vapour pressure dependence on temperature.

A new EOS for ethanol was also used to correlate our data, as well as the data from other authors with also good agreement supporting the fact that this apparatus provides good and accurate data.

## ***Paper I***

A.F. Cristino, S. Rosa, P. Morgado, A. Galindo, E. J. M. Filipe, A. M. F. Palavra and C. A. Nieto de Castro, *High-temperature vapour-liquid equilibrium for the water-alcohol systems and modeling with SAFT-VR: 1. Water-ethanol*, Fluid Phase Equilib. 341 (2013) 48-53  
doi:10.1016/j.fluid.2012.12.014

Note: The author of this thesis contribute to reassembling, testing of the equipment, to the vapour liquid equilibrium measurements of the pure components, data analysis, to the discussion and conclusions.

## ***Paper II***

A.F. Cristino, S. Rosa, P. Morgado, A. Galindo, E. J. M. Filipe, A. M. F. Palavra and C. A. Nieto de Castro, *High-temperature vapour-liquid equilibrium for the water-alcohol systems and modeling with SAFT-VR: 1. Water-1-propanol*, J. Chem. Thermodyn. 60 (2013) 15-18  
doi:10.1016/j.jct.2012.12.019

Note: The author of this thesis contribute to the vapour liquid equilibrium measurements, data analysis, to the discussion and conclusions.

## ***Paper III***

A.F. Cristino, P. Morgado, A. Galindo, E. J. M. Filipe, A. M. F. Palavra and C. A. Nieto de Castro, *High-temperature vapour-liquid equilibrium for ethanol-1-propanol mixtures and modeling with SAFT-VR*, Submitted to Fluid Phase Equilibria

Note: The author of this thesis contribute to the vapour liquid equilibrium measurements, data analysis, to the discussion and conclusions.



## **Chapter 6 – Conclusions and Future Perspectives**

This chapter summarizes the major conclusions from the research done in this Ph.D thesis and presents ideas that can be explore in the future, some of which that are already in course.

### **6.1. Overall Comments and Conclusions**

The water-alcohol system is of much interest in the context of distillation processes, and as such, a detailed understanding of its properties is crucial. A key to the design of new, more energy-efficient processes and solvents is the ability to predict thermophysical properties accurately. This was one of the overall aims of this work.

In chapter 4, a description of a flow apparatus for the measurement of the vapour-liquid equilibria was made. This apparatus originally constructed by Rosa *et al.* [1], was improved with new pressure transducers, new micro-metering valves and a new relief valve. These upgrades had the goal of an improvement of the accuracy of the pressure data and sampling. The evaluation and test of the apparatus was made with a well-studied alcohol, such as ethanol, since accurate data exists with the purpose of evaluate the problems inherent to a flow apparatus. These tests and evaluations, despite of having an analytical fundament, are primarily operator and experimental procedure dependent. Many conclusions were taken from these tests, but most important it was the establishment of a new experimental procedure.

The determination of the composition of the mixtures in vapour and liquid phases was performed with a density vs molar fraction calibration curve. The densimeters used for water + ethanol mixtures were calibrated using the classical method. However, for the remaining systems involving n-propanol the new densimeters were calibrated according the methodology described by Lampreia and Nieto de Castro [2], more reliable and accurate.

Measurements with the water-ethanol, water-1-propanol and ethanol-1-propanol systems at different temperatures were made and compared with literature data and with the SAFT-VR approach. For such known alcohols it was expected to find more accurate data in the literature. However for the chosen temperatures there wasn't available the amount of data expected. And when existing, some do not have the accuracy claimed. This tells us that this data is still used nowadays for designing but also that a lot of work need to be done in this area. The comparison of our results, obtained with the flow method, with literature suggests the quality of working conditions of the apparatus, as well as their accuracy.

The comparison of our results with SAFT-VR predictions, a well based equation of state, used by many authors as one of the best improvements of the originally SAFT theory, showed that it can predict the behaviour of the binary mixtures under study. It should be emphasized that in the calculations, the unlike interactions parameters were obtained from Lorentz-Berthelot [3] type combining rules. For the system ethanol + 1-propanol, an almost ideal solution, it was not necessary to use corrections to the binary mixing rules (equations 2.24 to 2.26) The good performance of the Lorentz-Berthelot combining rules reflects the similarity between the two studied substances. The theoretical results are thus true predictions. The only setback was the prediction for pure ethanol vapour pressure. In papers I and III, the theory has proven to overestimate the vapour pressure of pure ethanol. For this a coherence test was performed to the pure alcohols vapour pressures using the Wagner equation. The results show a good agreement between our data for the pure alcohols, previous experimental determinations [4-5] and the recent equation of state of Schroeder *et al.* [6] for ethanol. They also show that Wagner equation is one of the most effectives in modelling the vapour pressure

dependence on temperature, although minor corrections to the exponents are necessary near the critical point, as used by Schroeder *et al.* [6].

In order to obtain data for higher temperatures and pressures, a second apparatus was designed using the same flow technique. This apparatus capable of reaching 573.15K and 20MPa will offer the possibility of complementing the first one originating a larger range for pressure and temperature. The equilibrium cell was also redesigned in order to allow these thermodynamic studies. The materials (the sapphire window used in the cell, the gold o-rings and all the materials in the valves) used in this cell were also chosen very carefully in order to permit these higher values of temperature and pressure.

## **6.2. Future Perspectives**

The present work was a contribution for the scientific and industrial community of accurate vapour liquid equilibrium data for water and alcohol binary mixtures. Despite of the existing knowledge in this area, there is still immense work to be done, mainly because nowadays we can obtain more accurate data.

As mentioned earlier the cost of separation of two or more phases makes a significant contribution to the total cost of production. For the rational design of a typical separation process (for example, distillation), we need accurate thermodynamic properties of mixtures, i.e. the equilibrium concentrations of all components in all phases. This makes Thermodynamics the most important tool towards the optimization of one of the cornerstones of chemical engineering, the separation of fluid mixtures. This important fact enhances the necessity of continuing this work with the study of more binary mixtures containing both linear and branched alcohols. New equations of state can be applied to model our data. This work to be reported in the future.

This type of work can continue in the future with higher carbon chain alcohols, linear and branched, as well with mixtures of pinenes, in a logical connection to previous our in our group on density and specific heat [7-9].

One other focus of future work must be in mixtures with great impact in our industries and Ionic liquids (ILs) have become an important class of novel solvents.

Composed mostly by a combination of organic cations with organic or inorganic anions with alkyl chain, the possibility of changing this combination provides an excellent opportunity to adapt to a specific application becoming the most versatile solvents. Excellent reviews of ionic liquids on separation techniques [10] thermodynamic of non-aqueous mixtures [11], analytical applications [12] and in the field of catalysis [13] are available in the literature. However, much work remains to fully uncover the large potential of this novel class of liquids. For example, the technology of absorption heat pumps and refrigeration using absorption cooling cycles with ionic liquids has received growing attention in the past years. Classical working fluids, such as LiBr/H<sub>2</sub>O (which is corrosive and presents solidification problems) and H<sub>2</sub>O+NH<sub>3</sub> (which is toxic and an odor nuisance) systems have safety and environmental impacts that can be avoided simply by replacing them with IL-natural refrigerants (e.g; IL-H<sub>2</sub>O, IL-CO<sub>2</sub> and IL-NH<sub>3</sub>). This fact increases the need for information about the thermodynamic and transport properties of the mixtures of ILs with H<sub>2</sub>O, CO<sub>2</sub> or NH<sub>3</sub> for a better choice for new environmentally friendly absorption refrigerants. An extensive review on all these systems is currently under preparation, and will be published soon. Future work will include data for these binary mixtures important not only for the scientific community but also for the industry.

### **6.3. Bibliography**

- [1]. S.C.S. Rosa, C.A. Nieto de Castro, A.M.F. Palavra, Proceedings of 4th Asian Thermophysical Properties Conference (1995) 467–470
- [2]. I. M.S. Lampreia †, C. A. Nieto de Castro, J. Chem. Thermodyn. 43 (2011) 537–545
- [3]. Rowlinson, J. S., Swinton, F. L., Liquids and Liquid Mixtures, 3rd ed.; Butterworth Scientific, London, 1982

- [4]. A.F. Cristino, S. Rosa, P. Morgado, A. Galindo, E.J.M. Filipe, A.M.F. Palavra and C.A. Nieto de Castro, *Fluid Phase Equilib.* 341 (2013) 48-53
- [5]. A.F. Cristino, S. Rosa, P. Morgado, A. Galindo, E.J.M. Filipe, A.M.F. Palavra and C.A. Nieto de Castro, *J. Chem. Thermodyn.* 60 (2013) 15-18
- [6]. J. A. Schroeder, S. G. Penoncello, and J. S. Schroeder, *J. Phys. Chem. Ref. Data*, 43 (2014) 043102
- [7]. E. Langa, A. Palavra, C. A. Nieto de Castro, Ana Mainar, *J. Chem. Eng. Data* 56, (2011) 1709–1713
- [8]. E. Langa, A. Palavra, C. A. Nieto de Castro, Ana Mainar, *J. Chem. Thermodyn.* 48, (2012) 175-180
- [9]. E. Langa, A. Palavra, M. J. V. Lorenço, C. A. Nieto de Castro, Ana Mainar, *J. Chem Thermodyn.* 57 (2013) 493–499
- [10]. Berthod, M.J. Ruiz-Ángel, S. Carda-Brochv, *J. Chromatogr. A* 1184 (2008) 6–18
- [11]. Heintz, *J. Chem. Thermodyn.* 37 (2005) 525–535
- [12]. S. Pandey, *Anal. Chim. Acta* 556 (2006) 38–45
- [13]. H. Olivier-Bourbigou, L. Magna, D. Morvan, *Appl. Catal. A: Gen.* 373 (2010)

# Appendix 1 – Calibrations of the VLE apparatus #1

## A1.1. Platinum Resistance thermometer (PT100) from apparatus #1

The calibration of the PT100 of the VLE apparatus was conducted by EIA – Electrónica Aviónicos. The results from the calibration certificate are presented in the calibration certificate in Figure A. 1.

**E.I.A. - Electrónica Industrial de AVerca, Lda.**  
Certificação (INAC/EASA) PARTE 145 – PT.145.011

**Certificado de Calibração**  
(Continuação do Certificado N° 2996/12)

**Resultados**

| Valor do Padrão | Leitura no equipamento | Graus de liberdade efectivos | Factor de Expansão | Incerteza |
|-----------------|------------------------|------------------------------|--------------------|-----------|
| [°C]            | [Ω]                    | $\nu_{efec}$                 | k                  | [°C]      |
| 0,010           | 100,02963              | 223                          | 2,01               | ± 0,023   |
| 15,008          | 105,88770              | 175                          | 2,01               | ± 0,022   |
| 29,928          | 111,68534              | 91                           | 2,03               | ± 0,036   |
| 45,066          | 117,54695              | 121                          | 2,02               | ± 0,047   |
| 60,136          | 123,35228              | 96                           | 2,03               | ± 0,049   |
| 75,027          | 129,05760              | 97                           | 2,03               | ± 0,049   |
| 89,970          | 134,76243              | 105                          | 2,02               | ± 0,047   |
| 99,435          | 138,36441              | 71                           | 2,04               | ± 0,048   |
| 109,864         | 142,31731              | 75                           | 2,03               | ± 0,049   |
| 119,766         | 146,05841              | 76                           | 2,03               | ± 0,049   |
| 129,932         | 149,88749              | 77                           | 2,03               | ± 0,049   |
| 139,710         | 153,55812              | 77                           | 2,03               | ± 0,049   |
| 149,454         | 157,20304              | 77                           | 2,03               | ± 0,049   |
| 160,028         | 161,14796              | 96                           | 2,03               | ± 0,053   |
| 169,953         | 164,84350              | 102                          | 2,02               | ± 0,053   |

Observações:

$$T = \frac{-b + \sqrt{b^2 - 4 \times a \times (r_0 - v)}}{2 \times a}$$

$r_0=100,02545$   
 $a=-5,92115 \times 10^{-5}$   
 $b=0,391439$

A incerteza expandida apresentada está expressa pela incerteza-padrão multiplicada pelo factor de expansão apresentado na tabela acima, o qual para uma distribuição t com os graus de liberdade efectivos indicados corresponde a uma probabilidade de aproximadamente 95%. A incerteza de medição padrão foi calculada de acordo com o documento EA 4/02. A estabilidade do equipamento a longo prazo não foi considerada.

Figure A. 1 – Calibration certificate of the PT100 from apparatus #1

**A1.2. Manometers from apparatus #1**

In figures A.2 and A.3 the Calibration certificates of the pressure transducers from apparatus #1 are presented.

**GE Druck**

CALIBRATION CERTIFICATE  
POSITIVE PRESSURE

PAGE 1 of 1

|                              |                      |                               |                  |
|------------------------------|----------------------|-------------------------------|------------------|
| <u>UNIT UNDER TEST (UUT)</u> |                      | <u>CALIBRATOR INFORMATION</u> |                  |
| Manufacturer                 | : Druck              | Calibration Instrument        | : DPI510         |
| Type Number                  | : DPI 282            | Serial Number                 | : 0625/91-7      |
| Serial Number                | : 28205791           | (*1)Calibrated Against        | : UKAS Lab. 0221 |
| Sales Order Number           | : E01555.1.1         | Pressure Medium               | : Air            |
| Parameter Range              | : 0 to 4.000 bar abs | Uncertainty                   | : ±0.025% Rdg    |
| Calibration Date             | : 16 February 2011   | Calibration Instrument        | : DPI515         |
| Calibrated By                | : P Waddington       | Serial Number                 | : 51500954       |
| External Sensor Serial No.   | : 3277571            | (*1)Calibrated Against        | : UKAS Lab. 0221 |
|                              |                      | Pressure Medium               | : Air            |

AMBIENT CONDITIONS


Ambient Temperature (°C) : 23.3

PERFORMANCE DATA

| Actual Applied Value<br>bar | Unit Under Test Reading<br>bar (*2) | Unit Under Test Deviation<br>(*3) | Permissible Deviation<br>(*4) |
|-----------------------------|-------------------------------------|-----------------------------------|-------------------------------|
| 3.976                       | 3.976                               | +0.000 % fs                       | ± 0.050 % fs ± 1 digit        |
| 3.176                       | 3.176                               | +0.000 % fs                       | ± 0.050 % fs ± 1 digit        |
| 2.400                       | 2.399                               | -0.025 % fs                       | ± 0.050 % fs ± 1 digit        |
| 1.600                       | 1.599                               | -0.025 % fs                       | ± 0.050 % fs ± 1 digit        |
| 0.800                       | 0.799                               | -0.025 % fs                       | ± 0.050 % fs ± 1 digit        |
| 0.035                       | 0.035                               | +0.000 % fs                       | ± 0.050 % fs ± 1 digit        |

COMMENTS

Where fs = 4.000 bar

Certified by:  Date: 16. february. 11

NOTES

(\*1) This certificate provides traceability of measurement to recognised national standards and to units of measurement realised at the National Physical Laboratory or other recognised national standards laboratories.

(\*2) Actual recorded values. For specification, see Permissible Deviation column.

(\*3) Deviation calculated from UUT Reading minus Actual Applied Value.

(\*4) Non linearity, hysteresis and repeatability.

**Figure A. 2 – Calibration certificate of the pressure transducer with lower range (0-0.4MPa)**



GE Druck

CALIBRATION CERTIFICATE  
POSITIVE PRESSURE

PAGE 1 of 1

UNIT UNDER TEST (UUT)

Manufacturer : Druck  
 Type Number : DPI 282  
 Serial Number : 28205789  
 Sales Order Number : E01555.3.1  
 Parameter Range : 0 to 17.000 bar abs  
 Calibration Date : 01 March 2011  
 Calibrated By : P Waddington  
 External Sensor Serial No. : 3103713

CALIBRATOR INFORMATION

Calibration Instrument : DPI510  
 Serial Number : 0625/91-7  
 (\*1)Calibrated Against : UKAS Lab. 0221  
 Pressure Medium : Air  
 Uncertainty : ±0.025% Rdg  
  
 Calibration Instrument : DPI515  
 Serial Number : 51500954  
 (\*1)Calibrated Against : UKAS Lab. 0221  
 Pressure Medium : Air

AMBIENT CONDITIONS

Ambient Temperature (°C) : 20.7

PERFORMANCE DATA

| Actual Applied Value<br>bar | Unit Under Test Reading<br>bar (*2) | Unit Under Test Deviation<br>(*3) | Permissible Deviation<br>(*4) |
|-----------------------------|-------------------------------------|-----------------------------------|-------------------------------|
| 17.026                      | 17.026                              | +0.000 % fs                       | ± 0.050 % fs ± 1 digit        |
| 13.626                      | 13.626                              | +0.000 % fs                       | ± 0.050 % fs ± 1 digit        |
| 10.226                      | 10.224                              | -0.012 % fs                       | ± 0.050 % fs ± 1 digit        |
| 6.826                       | 6.829                               | +0.018 % fs                       | ± 0.050 % fs ± 1 digit        |
| 3.426                       | 3.428                               | +0.012 % fs                       | ± 0.050 % fs ± 1 digit        |
| 0.170                       | 0.167                               | -0.018 % fs                       | ± 0.050 % fs ± 1 digit        |

COMMENTS

Where fs = 17.000 bar

Certified by:

Date:

01. March. 11

NOTES

- (\*1) This certificate provides traceability of measurement to recognised national standards and to units of measurement realised at the National Physical Laboratory or other recognised national standards laboratories.
- (\*2) Actual recorded values. For specification, see Permissible Deviation column.
- (\*3) Deviation calculated from UUT Reading minus Actual Applied Value.
- (\*4) Non linearity, hysteresis and repeatability.

**Figure A. 3 – Calibration certificate of the pressure transducer with higher range (0-1.7MPa)**



### A1.1. PT100 from apparatus #2

The calibration of the PT100 of the VLE apparatus was conducted by the supplier. The results from the calibration certificate are presented in the calibration certificate in Figure A. 4.

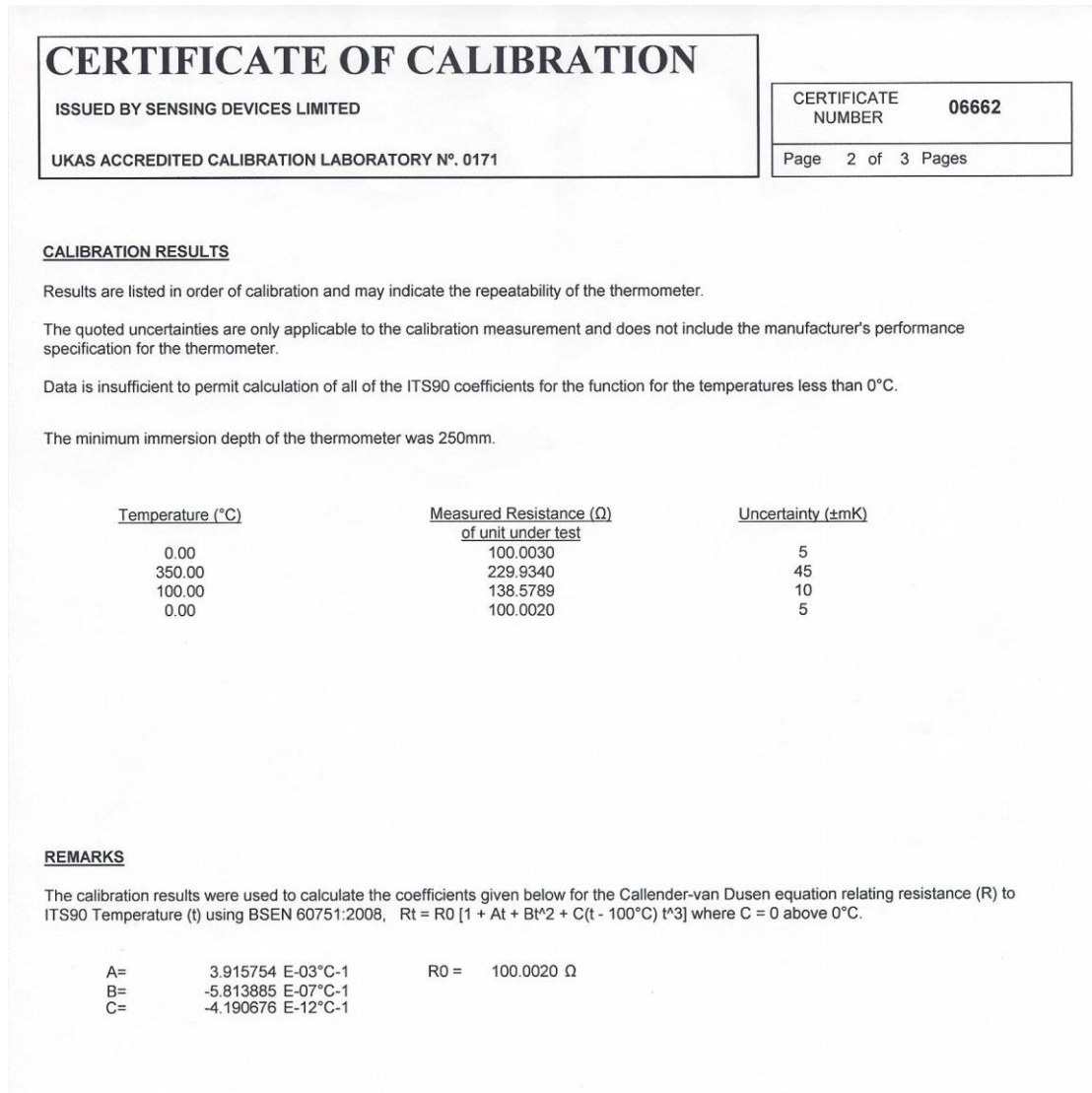


Figure A. 4 – Calibration certificate of the PT100 from apparatus #2

## Appendix 2 – Conversion of densities into molar fractions

The values of the density of the binary mixtures were obtained from published data and fitted to third order polynomials (equation A.1) in the molar fraction of ethanol within the range of the experimental measurements.

$$\text{molarfraction} = A + B \times \rho + C \times \rho^2 + D \times \rho^3 \quad \text{equation A. 1}$$

For the water-ethanol system a Portuguese standard was used [1] to convert densities into molar fractions at 293.2K. These results were divided into four ranges of density in order to minimize the error in the conversion. In table A 2.1 the results for the third order polynomial parameters for each density range is presented.

**Table A. 1 – Parameters for the polynomial equations of molar fraction vs density for water+ethanol**

| <i>A</i>  | <i>B</i>  | <i>C</i>  | <i>D</i>  | Density range        |
|-----------|-----------|-----------|-----------|----------------------|
| 83.9973   | -213.8998 | 177.6357  | -47.73650 | [0.998203; 0.97033 [ |
| 148.2090  | -466.9040 | 494.4409  | -175.8000 | [0.97033; 0.90688 [  |
| 59.43614  | -177.4131 | 179.7468  | -61.76374 | [0.90688; 0.82244]   |
| -101.5696 | 411.6026  | -538.7524 | 230.4754  | ] 0.82244; 0.78932]  |

The same method was applied to the water-1-propanol system, in this case using the results from Benson and Kiohara [2] at 303.2K (table A 2.2).

**Table A. 2 – Parameters for the polynomial equations of molar fraction vs density for water+1-propanol**

| <i>A</i> | <i>B</i>  | <i>C</i> | <i>D</i> | <i>Density range</i>  |
|----------|-----------|----------|----------|-----------------------|
| 31.35468 | -50.70319 | 0        | 19.82351 | [0.79547; 0.804885[   |
| 229.1745 | 754.8644  | 834.0296 | 308.8242 | [0.804885; 0.881865 [ |
| 78.0892  | -235.9090 | 239.71   | -81.8946 | [0.881865; 0.964113]  |
| -527.008 | 1625.274  | -1668.17 | 569.8976 | [0.964113; 0.995651]  |

For the ethanol+1-propanol system the results for the conversion at 293.2K were taken from the work of Cano-Gómez and Iglesias-Silva [3]. In this case a second order polynomial was applied to only one density range, for a better fitting. Table A 2.3 presents the polynomial parameters for the density range.

**Table A. 3 – Parameters for the polynomial equation of molar fraction vs density for ethanol+1-propanol**

| <i>A</i>  | <i>B</i> | <i>C</i>  | <i>Density range</i> |
|-----------|----------|-----------|----------------------|
| -331.5120 | 908.0048 | -616.5830 | [0.79013;0.80358 [   |

### A 2.1. Bibliography

- [1]. NP-753, Norma Portuguesa (Portuguese Standard), 1969
- [2]. G.C. Benson, O. Kiohara, J. Sol. Chem. 9 (1980) 791–804.
- [3]. J.J. Cano-Gómez and G.A. Iglesias-Silva, J. Chem. & Eng. Data, 57 (2012) 2560-2567

## Appendix 3 – Evaluation of the stability of the air bath of VLE#1

In tables A. 4 and A. 5 the results from the evaluation of the stability of the air bath of VLE apparatus #1 is presented.

**Table A. 4– Stability of the air bath at 296,55K with or without ventilation and with or without filling with steel mesh**

| <b>Filling</b>    | <b>RTD</b>          | <b>1</b> | <b>2</b> | <b>3</b> | <b>4</b> | <b>5</b> | <b>6</b> |
|-------------------|---------------------|----------|----------|----------|----------|----------|----------|
| <b>No filling</b> | room temperature    | 296.55   | 296.55   | 296.55   | 296.55   | 296.55   | 296.55   |
|                   | standard            | 296.85   | 296.65   | 296.55   | 297.95   | 295.55   | 297.95   |
|                   | with ventilation    | 297.25   | 297.75   | 297.25   | 297.95   | 297.35   | 297.85   |
|                   | without ventilation | 297.65   | 297.85   | 297.75   | 297.95   | 297.75   | 297.85   |
| <b>20 mesh</b>    | standard            | 296.85   | 296.65   | 296.55   | 297.95   | 295.55   | 297.95   |
|                   | with ventilation    | 293.25   | 293.95   | 293.55   | 293.75   | 293.85   | 294.55   |
|                   | without ventilation | 294.75   | 295.05   | 294.85   | 294.95   | 294.95   | 294.75   |
| <b>40 mesh</b>    | standard            | 296.85   | 296.65   | 296.55   | 297.95   | 295.55   | 297.95   |
|                   | with ventilation    | 293.45   | 294.15   | 293.65   | 293.65   | 293.75   | 294.85   |
|                   | without ventilation | 294.85   | 296.35   | 296.25   | 295.95   | 294.95   | 297.55   |

**Table A. 5- Stability of the air bath at 423.15K with or without filling with steel mesh**

| <b>RTD</b>        | <b>1</b> | <b>2</b> | <b>3</b> | <b>4</b> | <b>5</b> | <b>6</b> |
|-------------------|----------|----------|----------|----------|----------|----------|
| <b>standard</b>   | 423.15   | 423.15   | 423.15   | 423.15   | 423.15   | 423.15   |
| <b>no filling</b> | 426.65   | 421.05   | 427.95   | 425.05   | 428.35   | 399.45   |
| <b>20 mesh</b>    | 428.75   | 421.55   | 431.95   | 425.65   | 429.35   | 396.25   |
| <b>40 mesh</b>    | 427.95   | 422.15   | 427.55   | 426.15   | 425.65   | 392.55   |